Efficient adaptive stochastic Galerkin methods for parametric operator equations

DOI:
10.1137/15M1027048

Document Version
Accepted author manuscript

EFFICIENT ADAPTIVE STOCHASTIC GALERKIN METHODS FOR PARAMETRIC OPERATOR EQUATIONS

ALEX BESPALOV[†] AND DAVID SILVESTER[‡]

Abstract. This paper is concerned with the design and implementation of efficient solution algorithms for elliptic PDE problems with correlated random data. The energy orthogonality that is built into stochastic Galerkin approximations is cleverly exploited to give an innovative energy error estimation strategy that utilizes the tensor product structure of the approximation space. An associated error estimator is constructed and shown theoretically and numerically to be an effective mechanism for driving an adaptive refinement process. The codes used in the numerical studies are available online.

Key words. stochastic Galerkin methods, stochastic finite elements, PDEs with random data, error estimation, a posteriori error analysis, adaptive methods, parametric operator equations

AMS subject classifications. 35R60, 65C20, 65N30, 65N15.

1. Introduction. Stochastic Galerkin approximation methods have emerged over the last decade as an efficient alternative to sampling methods for computing solutions (and associated quantities of interest) when studying linear elliptic PDE problems with correlated random data. A typical strategy is to combine conventional (h-) finite element approximation on the spatial domain with spectral (p-) approximation on a finite-dimensional manifold in the (stochastic) parameter domain. The development of good/optimal adaptive refinement strategies remains an open question however. It is highlighted in our previous work [4] as well as by other researchers: notably Le Maître and collaborators [13], [14], [15], Wan & Karniadakis [19], [20], and Butler and collaborators [6], [5]. The strategy that is developed herein is similar in spirit to that developed by Eigel et al. [7], but it is novel in that a posteriori estimates of the error reduction in the energy norm (rather than the error itself) are used to guide the adaptivity process.

An outline of the paper is as follows. Sections 2 and 3 set the problem of interest within the general framework of parametric operator equations with a potentially infinite-dimensional parameter space. The new error estimator is identified in Section 4. The estimator is shown to be reliable and efficient, and its properties are established that prove useful when individual error components are used to drive adaptive refinement. A specific implementation of an adaptive refinement strategy is described in section 5, and a set of numerical experiments that illustrate the effectiveness of the strategy is presented in section 6. One notable feature is that our software implementation is not limited to the lowest-order conforming spatial approximation—this means that we can solve spatially-regular problems to high accuracy with just a few adaptive refinement steps.

2. Parametric operator equations. Our setting is the framework established in the review article of Schwab & Gittelson [17]. It is reiterated for completeness in this section. Our notation is identical to that used in the precursor paper [4]. Let Γ be a topological space and let H be a separable Hilbert space over $\mathbb{R}$ with natural

[†]School of Mathematics, University of Birmingham, Edgbaston, Birmingham B15 2TT, UK, a.bespalov@bham.ac.uk

[‡]School of Mathematics, University of Manchester, Oxford Road, Manchester, M13 9PL, UK, d.silvester@manchester.ac.uk

norm $\|\cdot\|_H$. We denote the dual space of H by H' and the corresponding duality pairing by $\langle\cdot,\cdot\rangle$. Our focus is on the following parametric operator equation

$$A(y)\,u(y) = f(y) \qquad \forall\, y \in \Gamma, \tag{2.1}$$

where $A : \Gamma \to \mathcal{L}(H, H')$ and $f : \Gamma \to H'$ are given continuous maps defining for each $y \in \Gamma$ a symmetric bounded linear operator in $\mathcal{L}(H, H')$ and a linear functional in H', respectively. We assume that $A(y)$ has a bounded inverse for all $y \in \Gamma$ so that (2.1) has a unique solution $u : \Gamma \to H$ which is a continuous map. Our aim is to use stochastic finite element techniques to solve PDE problems with random data. Accordingly, we suppose that $\Gamma := \prod_{m=1}^{\infty} \Gamma_m$, with Γ_m being bounded intervals in $\mathbb{R}$, and assume that π is a product measure. In this case the elements of Γ are vectors, denoted by $\mathbf{y} = (y_1, y_2, \ldots) \in \Gamma$, and $\pi(\mathbf{y}) := \prod_{m=1}^{\infty} \pi_m(y_m)$, where π_m is a measure on $\big(\Gamma_m, \mathcal{B}(\Gamma_m)\big)$ with $\mathcal{B}(\Gamma_m)$ representing the Borel σ-algebra on Γ_m. We define V to be the Bochner space $L^2_\pi(\Gamma; H)$ with associated norm

$$\|\cdot\|_V := \left(\int_\Gamma \|\cdot\|_H^2 \,\mathrm{d}\pi(\mathbf{y})\right)^{1/2}.$$

This leads to the following weak formulation of (2.1): find $u \in V$ such that

$$B(u, v) = F(v) \qquad \forall\, v \in V, \tag{2.2}$$

with the symmetric bilinear form and the linear functional

$$B(u, v) := \int_\Gamma \langle A(\mathbf{y})u(\mathbf{y}), v(\mathbf{y})\rangle \,\mathrm{d}\pi(\mathbf{y}) \;\text{ and }\; F(v) := \int_\Gamma \langle f(\mathbf{y}), v(\mathbf{y})\rangle \,\mathrm{d}\pi(\mathbf{y}). \tag{2.3}$$

To ensure that (2.2) is well posed, we will assume that $f \in L^2_\pi(\Gamma; H')$, the operator $A(\mathbf{y})$ is positive definite for all $\mathbf{y} \in \Gamma$, and that there exist positive constants $\alpha_{\min}$ and $\alpha_{\max}$ such that

$$\|A(\mathbf{y})\|_{\mathcal{L}(H,H')} \le \alpha_{\max}, \quad \|A(\mathbf{y})^{-1}\|_{\mathcal{L}(H',H)} \le \alpha_{\min}^{-1} \quad \forall\, \mathbf{y} \in \Gamma. \tag{2.4}$$

It is evident that $B(\cdot,\cdot)$ defines an inner product in V and that it induces an *energy* norm $\|v\|_B := (B(v, v))^{1/2}$ that is equivalent to $\|v\|_V$.

The key assumption that is needed for our error estimation strategy is that $A(\mathbf{y})$ *is a linear function of the parameters*; that is, taking the form

$$A(\mathbf{y}) = A_0 + \sum_{m=1}^{\infty} y_m A_m \qquad \forall\, \mathbf{y} \in \Gamma, \tag{2.5}$$

where A_0 is symmetric positive definite and the operators $A_m \in \mathcal{L}(H, H')$ are symmetric for $m \in \mathbb{N}$. To ensure well-posedness in the sense of (2.4) we follow Gittelson [11, section 1] by assuming (with justification, see later in this section) that there exists a constant $\tau \in [0, 1)$ such that for all $\mathbf{y} \in \Gamma$,

$$\left|\left\langle \sum_{m=1}^{\infty} y_m A_m v, v \right\rangle\right| \le \tau \,\langle A_0 v, v\rangle \qquad \forall\, v \in H.$$

Substituting (2.5) into (2.3) allows us to split $B(\cdot,\cdot)$ and rewrite (2.2) as

$$B_0(u, v) + \sum_{m=1}^{\infty} B_m(u, v) = F(v) \qquad \forall\, v \in V,$$

where the component bilinear forms $B_m(\cdot,\cdot)$ for $m \in \mathbb{N}_0$ are defined as

$$B_0(u,v) := \int_\Gamma \langle A_0 u(\mathbf{y}), v(\mathbf{y})\rangle \,\mathrm{d}\pi(\mathbf{y}), \tag{2.6}$$

$$B_m(u,v) := \int_\Gamma \langle A_m u(\mathbf{y}), v(\mathbf{y})\rangle \, y_m \,\mathrm{d}\pi(\mathbf{y}) \qquad \forall\, m \in \mathbb{N}.$$

The assumptions on A_0 imply that the bilinear form $B_0(\cdot,\cdot)$ defines an inner product in V which induces the norm $\|v\|_{B_0} := (B_0(v,v))^{1/2}$ which is also equivalent to $\|v\|_V$. This implies that there exist positive constants λ, Λ, such that

$$\lambda\, B(v,v) \le B_0(v,v) \le \Lambda\, B(v,v) \qquad \forall\, v \in V. \tag{2.7}$$

To give a concrete example of the abstract problem (2.2) we let $D \subset \mathbb{R}^2$ be a Lipschitz domain with polygonal boundary ∂D, and consider the homogeneous Dirichlet problem for the steady-state diffusion equation with a random, spatially varying diffusion coefficient. More precisely, it is assumed that the diffusion coefficient $a = a(\mathbf{x}, \boldsymbol{\xi})$ is a second-order correlated random field that can be written as a function of a multivariate random variable $\boldsymbol{\xi} = (\xi_1, \xi_2, \ldots)$ and that the right-hand side function $f = f(\mathbf{x})$ is deterministic. It is known (see e.g., [10, 12, 2, 17]), that we may rewrite this problem in the following parametric form

$$\begin{aligned} -\nabla\cdot(a(\mathbf{x},\mathbf{y})\nabla u(\mathbf{x},\mathbf{y})) &= f(\mathbf{x}), \qquad \mathbf{x} \in D,\ \mathbf{y} \in \Gamma, \\ u(\mathbf{x},\mathbf{y}) &= 0, \qquad \mathbf{x} \in \partial D,\ \mathbf{y} \in \Gamma, \end{aligned} \tag{2.8}$$

where $\Gamma := \prod_{m=1}^{\infty} [-1,1]$, with the diffusion coefficient represented as

$$a(\mathbf{x},\mathbf{y}) = a_0(\mathbf{x}) + \sum_{m=1}^{\infty} a_m(\mathbf{x})\, y_m, \quad \mathbf{x} \in D,\ \mathbf{y} \in \Gamma, \tag{2.9}$$

and with the series converging uniformly in $L^\infty(D)$.

The parameter-free term $a_0(\mathbf{x})$ in (2.9) typically represents the mean: that is,

$$a_0(\mathbf{x}) = \int_\Gamma a(\mathbf{x},\mathbf{y})\,\mathrm{d}\pi(\mathbf{y}) = \mathbb{E}[a](\mathbf{x}), \quad \mathbf{x} \in D.$$

This is true, for example, for Karhunen-Loève expansions since in that case each y_m in (2.9) is the image of a mean-zero random variable and so

$$\int_{\Gamma_m} y_m \, d\pi_m(y_m) = 0. \tag{2.10}$$

If $\Gamma_m = [-1,1]$ and we additionally assume that the measure π_m is symmetric, then (2.10) always holds. To express (2.8) in the form (2.1), we let $H := H_0^1(D)$, $f(\mathbf{y}) := f \in H^{-1}(D)$ for all $\mathbf{y} \in \Gamma$, and define the operator $A(\mathbf{y}) \in \mathcal{L}(H_0^1(D), H^{-1}(D))$ for all $\mathbf{y} \in \Gamma$ by the following identity

$$\langle A(\mathbf{y})v, w\rangle := \int_D a(\mathbf{x},\mathbf{y})\,\nabla v(\mathbf{x})\cdot\nabla w(\mathbf{x})\,\mathrm{d}\mathbf{x} \quad \forall\, v, w \in H_0^1(D). \tag{2.11}$$

Then, due to (2.9), the operator $A(\mathbf{y})$ admits decomposition (2.5) with A_0 and A_m, $m \in \mathbb{N}$, defined by

$$\langle A_0 v, w\rangle := \int_D a_0(\mathbf{x})\,\nabla v(\mathbf{x})\cdot\nabla w(\mathbf{x})\mathrm{d}\mathbf{x} \quad \forall\, v, w \in H_0^1(D), \tag{2.12}$$

$$\langle A_m v, w\rangle := \int_D a_m(\mathbf{x})\,\nabla v(\mathbf{x})\cdot\nabla w(\mathbf{x})\mathrm{d}\mathbf{x} \quad \forall\, v, w \in H_0^1(D).$$

To ensure a well-posed problem we assume that $a_0(\mathbf{x}) \in L^\infty(D)$ is uniformly bounded away from zero, i.e.,

$$\exists\, \alpha_0^{\min},\, \alpha_0^{\max} > 0 \;\text{ such that }\; \alpha_0^{\min} \le a_0(\mathbf{x}) \le \alpha_0^{\max} \;\text{ a.e. in } D. \tag{2.13}$$

We also assume that $a_m(\mathbf{x}) \in L^\infty(D)$, $m \in \mathbb{N}$, and

$$\tau := \frac{1}{\alpha_0^{\min}} \sum_{m=1}^{\infty} \|a_m\|_{L^\infty(D)} < 1. \tag{2.14}$$

On the one hand, (2.14) ensures convergence of the series in (2.5) uniformly in $\mathbf{y}$, see [17, Lemma 2.21]. On the other hand, (2.14) together with (2.13) imply bounded invertibility of $A(\mathbf{y})$ for all $\mathbf{y} \in \Gamma$ (and, hence, unique solvability of (2.1)) and inequalities (2.4) hold with

$$\alpha_{\max} := \alpha_0^{\max}(1+\tau) \quad \text{and} \quad \alpha_{\min} := \alpha_0^{\min}(1-\tau),$$

see [17, Proposition 2.22]. Note that this implies that

$$\alpha_{\min} < \alpha_0^{\min} \le \alpha_0^{\max} < \alpha_{\max},$$

and hence the constants λ and Λ in (2.7) satisfy $\lambda < 1 < \Lambda$.

3. Discrete formulations. The weak problem (2.2) will be discretized by constructing a finite-dimensional subspace $V_N \subset V$ and using Galerkin projection onto V_N. This defines a unique element $u_N \in V_N$ satisfying

$$B(u_N, v) = F(v) \qquad \forall\, v \in V_N. \tag{3.1}$$

Our goal is to design an algorithm for adaptive selection of a sequence of finite dimensional subspaces $V_N \subset V$ such that a specified tolerance is met by the Galerkin solution $u_N \in V_N$. This involves two essential ingredients. First, we need to find a reliable and efficient estimator for the approximation error $u - u_N$ (measured in an appropriate norm). Second, we need to develop an effective strategy for adaptive refinement of stochastic Galerkin approximations.

We will exploit the tensor product structure of the Galerkin approximation space $V_N = X \otimes \mathcal{P}_{\mathfrak{P}} \subset H \otimes L^2_\pi(\Gamma) \simeq V$ by constructing finite-dimensional subspaces $X \subset H$ and $\mathcal{P}_{\mathfrak{P}} \subset L^2_\pi(\Gamma)$ independently of each other. For the approximation on the parameter domain Γ, let $\{P_n^m\}_{n\in\mathbb{N}_0}$ denote the set of univariate polynomials on Γ_m that are orthonormal with respect to the measure π_m. Note that for any polynomial P_n^m, the index n refers to the polynomial degree and we denote by c_n^m the leading coefficient of P_n^m. The set $\{P_n^m\}_{n\in\mathbb{N}_0}$ is an orthonormal basis of $L^2_{\pi_m}(\Gamma_m)$. Moreover, it is well known that these polynomials satisfy the following three-term recurrence (e.g., see [9, 18]):

$$P_0^m \equiv 1; \quad \beta_n^m P_{n+1}^m(t) = (t - \alpha_n^m)P_n^m(t) - \beta_{n-1}^m P_{n-1}^m(t), \quad n \in \mathbb{N},\ t \in \Gamma_m, \tag{3.2}$$

where

$$\alpha_n^m = \int_{\Gamma_m} t\,(P_n^m(t))^2\,\mathrm{d}\pi_m(t) \text{ for } n \in \mathbb{N} \quad \text{and} \quad \beta_n^m = \frac{c_n^m}{c_{n+1}^m} \text{ for } n \in \mathbb{N}_0.$$

Note that if $\Gamma_m = [-1, 1]$ and the measure π_m is symmetric then $\alpha_n^m = 0$ in (3.2). The recurrence formula (3.2) will be a crucial tool in the analysis of the error estimator in section 4.2.

To construct an orthonormal basis of multivariate polynomials for $L^2_\pi(\Gamma)$, we introduce the following set of finitely supported sequences:

$$\mathfrak{J} := \big\{\nu = (\nu_1, \nu_2, \ldots) \in \mathbb{N}_0^{\mathbb{N}};\ \#\ \text{supp}\ \nu < \infty\big\},$$

where $\text{supp}\ \nu := \{m \in \mathbb{N};\ \nu_m \neq 0\}$ for any $\nu \in \mathbb{N}_0^{\mathbb{N}}$. We will call $\mathfrak{J}$ and any of its subsets the *index sets*. The countable set of tensor product polynomials defined by $P_\nu(\mathbf{y}) = \prod_{m=1}^\infty P_{\nu_m}^m(y_m)$, $\forall\,\nu \in \mathfrak{J}$ forms an orthonormal basis of $L^2_\pi(\Gamma)$. Since $P_0^m(y_m) \equiv 1$ for any $m \in \mathbb{N}$, we have the characterization

$$P_\nu(\mathbf{y}) = \prod_{m \in \text{supp}\ \nu} P_{\nu_m}^m(y_m), \quad \forall\,\nu \in \mathfrak{J}. \tag{3.3}$$

Given a finite index set $\mathfrak{P} \subset \mathfrak{J}$, the space of multivariate polynomials $\mathcal{P}_\mathfrak{P} := \text{span}\{P_\nu;\ \nu \in \mathfrak{P}\}$ defines a finite-dimensional subspace of $L^2_\pi(\Gamma)$. Each polynomial $P_\nu \in \mathcal{P}_\mathfrak{P}$ is a function of a finite number of the parameters y_m, $m \in \mathbb{N}$, and the corresponding Galerkin approximation space is given by

$$V_N = V_{X\mathfrak{P}} := X \otimes \mathcal{P}_\mathfrak{P}, \tag{3.4}$$

where X is a finite-dimensional subspace of H and $\mathfrak{P}$ is a finite subset of the index set $\mathfrak{J}$. We will implicitly assume that $\mathfrak{P}$ always contains the zero-index $\mathbf{0} = (0, 0, \ldots)$. We note that the choice of the index set $\mathfrak{P}$ for $\mathcal{P}_\mathfrak{P}$ determines both the number of "active" parameters y_m in the polynomial approximation on Γ, and the polynomial degrees in these "active" parameters.

Given the construction (3.4), it will be convenient to rewrite (3.1) as follows: find $u_{X\mathfrak{P}} \in V_{X\mathfrak{P}}$ satisfying

$$B(u_{X\mathfrak{P}}, v) = F(v) \qquad \forall\, v \in V_{X\mathfrak{P}}. \tag{3.5}$$

The approximation provided by (3.5) can be improved by enriching the subspace $V_{X\mathfrak{P}}$. This can be done by enriching the finite-dimensional subspace $X \subset H$ and/or the polynomial space $\mathcal{P}_\mathfrak{P} \subset L^2_\pi(\Gamma)$. To this end, suppose that X^* is a finite-dimensional subspace of H such that $X^* \supset X$. For example, in finite element methods, X^* could be obtained from X by adding new basis functions corresponding to nodes introduced by mesh refinement. Then, X^* can be decomposed as

$$X^* = X \oplus Y, \tag{3.6}$$

where $Y \subset H$ and $X \cap Y = \{0\}$. The subspace Y will be called the *detail space*. We observe that, since $\langle A_0 \cdot, \cdot\rangle$ defines an inner product in H and $X \cap Y = \{0\}$, there exists a constant $\gamma \in [0, 1)$ such that the strengthened Cauchy–Schwarz inequality holds (see e.g., Eijkhout & Vassilevski [8]). That is,

$$|\langle A_0 u_X, v_Y\rangle| \leq \gamma\,\langle A_0 u_X, u_X\rangle^{1/2}\,\langle A_0 v_Y, v_Y\rangle^{1/2} \qquad \forall\, u_X \in X,\ \forall\, v_Y \in Y. \tag{3.7}$$

On the parameter domain Γ, we introduce an enriched polynomial space $\mathcal{P}_{\mathfrak{P}^*}$ corresponding to a larger index set $\mathfrak{P}^* \supset \mathfrak{P}$. Thus, $\mathfrak{P}^* = \mathfrak{P} \cup \mathfrak{Q}$ with $\mathfrak{Q} \subset \mathfrak{I}$ such that $\mathfrak{P} \cap \mathfrak{Q} = \emptyset$. We will call $\mathfrak{Q}$ the *detail index set*. Then, $\mathcal{P}_{\mathfrak{P}^*}$ can be decomposed as

$$\mathcal{P}_{\mathfrak{P}^*} = \mathcal{P}_{\mathfrak{P}} \oplus \mathcal{P}_{\mathfrak{Q}}, \qquad \mathcal{P}_{\mathfrak{P}} \cap \mathcal{P}_{\mathfrak{Q}} = \{0\}. \tag{3.8}$$

The decomposition in (3.8) is orthogonal with respect to the measure π. That is,

$$\int_\Gamma P_\nu(\mathbf{y})\, P_\mu(\mathbf{y})\, \mathrm{d}\pi(\mathbf{y}) = 0 \qquad \forall\, \nu \in \mathfrak{P},\ \forall\, \mu \in \mathfrak{Q}. \tag{3.9}$$

We use the finite-dimensional subspaces X, $Y \subset H$ and the index sets $\mathfrak{P}$, $\mathfrak{Q} \subset \mathfrak{I}$ to define the following finite-dimensional subspaces of V:

$$V_{Y\mathfrak{P}} := Y \otimes \mathcal{P}_{\mathfrak{P}}, \quad V_{X\mathfrak{Q}} := X \otimes \mathcal{P}_{\mathfrak{Q}}. \tag{3.10}$$

Note that for any finite index set $\mathfrak{P} \subset \mathfrak{I}$, the subspaces $V_{X\mathfrak{P}}$, $V_{Y\mathfrak{P}} \subset V$ are such that the strengthened Cauchy–Schwarz inequality

$$|B_0(u,v)| \le \gamma\, \|u\|_{B_0}\, \|v\|_{B_0} \qquad \forall\, u \in V_{X\mathfrak{P}},\ \forall\, v \in V_{Y\mathfrak{P}} \tag{3.11}$$

holds with the same constant $\gamma \in [0,1)$ as in the strengthened Cauchy–Schwarz inequality (3.7) for the subspaces X, $Y \subset H$. This fact is due to the orthonormality of the polynomials in $\mathcal{P}_{\mathfrak{P}}$ (see [4, Lemma 3.1] for the proof of (3.11)).

We will define the *enriched* finite-dimensional subspace of V as the space[1]

$$V^*_{X\mathfrak{P}} := V_{X^*\mathfrak{P}} \oplus V_{X\mathfrak{Q}} = V_{X\mathfrak{P}} \oplus V_{Y\mathfrak{P}} \oplus V_{X\mathfrak{Q}}, \tag{3.12}$$

where $V_{X^*\mathfrak{P}} := X^* \otimes \mathcal{P}_{\mathfrak{P}}$, and $V_{Y\mathfrak{P}}$, $V_{X\mathfrak{Q}}$ are defined by (3.10). Thus, the original subspace $V_{X\mathfrak{P}}$ is enriched by adding new basis functions $\phi_\nu P_\nu(\mathbf{y})$, where either $\nu \in \mathfrak{P}$ and $\phi_\nu \in Y$ (basis functions in $V_{Y\mathfrak{P}}$), or $\nu \in \mathfrak{Q}$ and $\phi_\nu \in X$ (basis functions in $V_{X\mathfrak{Q}}$). Next, let $u^*_{X\mathfrak{P}} \in V^*_{X\mathfrak{P}}$ be the Galerkin projection onto the enriched subspace $V^*_{X\mathfrak{P}}$, so that

$$B(u^*_{X\mathfrak{P}}, v) = F(v) \qquad \forall\, v \in V^*_{X\mathfrak{P}}. \tag{3.13}$$

The approximation $u^*_{X\mathfrak{P}} \in V^*_{X\mathfrak{P}}$ generated by (3.13) is not worse than the approximation $u_{X\mathfrak{P}} \in V_{X\mathfrak{P}}$, in the following sense:

$$\|u - u^*_{X\mathfrak{P}}\|_B = \inf_{v \in V^*_{X\mathfrak{P}}} \|u - v\|_B \le \|u - u_{X\mathfrak{P}}\|_B. \tag{3.14}$$

We will assume, as is commonly done in nonparametric a posteriori error analysis, that the following stronger property holds.

ASSUMPTION 3.1. (saturation assumption). *Let $u \in V$ solve* (2.2)*, and let $u_{X\mathfrak{P}} \in V_{X\mathfrak{P}}$ and $u^*_{X\mathfrak{P}} \in V^*_{X\mathfrak{P}} \supset V_{X\mathfrak{P}}$ be two Galerkin approximations satisfying* (3.5) *and* (3.13)*, respectively. We assume that there exists a constant $\beta \in [0,1)$ such that*

$$\|u - u^*_{X\mathfrak{P}}\|_B \le \beta\, \|u - u_{X\mathfrak{P}}\|_B. \tag{3.15}$$

[1] This enriched space is smaller than the enriched space $V^*_{X\mathfrak{P}}$ that was analyzed in [4].

4. A posteriori error estimation. A new a posteriori estimator for the discretization error $e := u - u_{X\mathfrak{P}} \in V$ will be developed in this section. Using (2.2), we have

$$B(e, v) = F(v) - B(u_{X\mathfrak{P}}, v) \qquad \forall\, v \in V. \tag{4.1}$$

Following [4] we can approximate the error $e \in V$ by using the bilinear form $B_0(\cdot,\cdot)$ given by (2.6) instead of $B(\cdot,\cdot)$ on the left-hand side of (4.1), and by discretizing the resulting identity via Galerkin projection onto the enriched subspace $V^*_{X\mathfrak{P}}$ given by (3.12). This leads to the error estimator $e^*_0 \in V^*_{X\mathfrak{P}}$ satisfying

$$B_0(e^*_0, v) = F(v) - B(u_{X\mathfrak{P}}, v) \qquad \forall\, v \in V^*_{X\mathfrak{P}}. \tag{4.2}$$

We emphasize the advantage of using the B_0 inner product from the point of view of linear algebra. Indeed, since B_0 incorporates only the parameter-free part of the operator $A(\mathbf{y})$, it invariably leads to a block diagonal system matrix. Calculations can then be decomposed into multiple problems each having the dimension of a finite-dimensional subspace of H (either $X^* \subset H$ or $X \subset H$). Effectively, this means that the contributions to discretization error arising from the choice of X and $\mathfrak{P}$ are decoupled in the error estimator e^*_0. More precisely (cf. (3.12)),

$$e^*_0 = e_{X^*\mathfrak{P}} + e_{X\mathfrak{Q}} \quad \text{and} \quad \|e^*_0\|_{B_0} = \Big(\|e_{X^*\mathfrak{P}}\|^2_{B_0} + \|e_{X\mathfrak{Q}}\|^2_{B_0}\Big)^{1/2},$$

where the contributing *spatial* error estimator $e_{X^*\mathfrak{P}} \in V_{X^*\mathfrak{P}}$ and the *parameter* error estimator $e_{X\mathfrak{Q}} \in V_{X\mathfrak{Q}}$ satisfy, respectively,

$$B_0(e_{X^*\mathfrak{P}}, v) = F(v) - B(u_{X\mathfrak{P}}, v) \qquad \forall\, v \in V_{X^*\mathfrak{P}}, \tag{4.3a}$$

$$B_0(e_{X\mathfrak{Q}}, v) = F(v) - B(u_{X\mathfrak{P}}, v) \qquad \forall\, v \in V_{X\mathfrak{Q}}. \tag{4.3b}$$

Note that these estimators are computable because $\mathfrak{P}$ and $\mathfrak{Q}$ are finite index sets.

The following result is an immediate consequence of Propositions 4.1 and 4.2 in [4]. It establishes the relation between the true error e in (4.1) and the estimator e^*_0 satisfying (4.2).

PROPOSITION 4.1. *Suppose that (saturation) Assumption* 3.1 *holds for the solution u to* (2.2)*. Then, the estimator e^*_0 defined by* (4.2) *satisfies*

$$\sqrt{\lambda}\,\|e^*_0\|_{B_0} \le \|e\|_B \le \frac{\sqrt{\Lambda}}{\sqrt{1-\beta^2}}\,\|e^*_0\|_{B_0}, \tag{4.4}$$

where λ, Λ are the constants in (2.7) *and $\beta \in [0,1)$ is the constant in* (3.15)*.*

Note that the computational cost associated with solving (4.3a) can be significantly higher than the cost of solving (4.3b), because the full enhanced subspace $X^* \subset H$ is used in (4.3a). In order to avoid this, we can further exploit the decomposition of the enriched space $V^*_{X\mathfrak{P}}$ in (3.12) and perform computations on a lower-dimensional space. Indeed, instead of $e_{X^*\mathfrak{P}}$ in (4.3a) we can compute the error estimator $e_{Y\mathfrak{P}} \in V_{Y\mathfrak{P}}$ satisfying

$$B_0(e_{Y\mathfrak{P}}, v) = F(v) - B(u_{X\mathfrak{P}}, v) \qquad \forall\, v \in V_{Y\mathfrak{P}}. \tag{4.5}$$

Finally, combining the estimators $e_{Y\mathfrak{P}}$ and $e_{X\mathfrak{Q}}$ defined by (4.5) and (4.3b) gives the following estimate for the overall discretization error $\|e\|_B$:

$$\eta := \left(\|e_{Y\mathfrak{P}}\|_{B_0}^2 + \|e_{X\mathfrak{Q}}\|_{B_0}^2\right)^{1/2}. \tag{4.6}$$

Note that $B_0(e_{Y\mathfrak{P}}, e_{X\mathfrak{Q}}) = 0$ due to the orthogonality (3.9) of polynomial spaces $\mathcal{P}_{\mathfrak{P}}$ and $\mathcal{P}_{\mathfrak{Q}}$ with respect to the measure π. Therefore

$$\eta = \|e_{Y\mathfrak{P}} + e_{X\mathfrak{Q}}\|_{B_0}. \tag{4.7}$$

The connection between η and $\|e_0^*\|_{B_0}$ is established in the next lemma.

LEMMA 4.1. *Let $e_0^* \in V_{X\mathfrak{P}}^*$ be defined by* (4.2). *Then the error estimate η defined by* (4.6) *satisfies*

$$\eta \le \|e_0^*\|_{B_0} \le \frac{1}{\sqrt{1-\gamma^2}}\,\eta, \tag{4.8}$$

where $\gamma \in [0,1)$ is the constant in the strengthened Cauchy–Schwarz inequality (3.7) *for the subspaces $X, Y \subset H$.*

Proof. The proof is very similar to that of Lemma 4.1 in [4] and so we only outline the main steps. Since $V_{X\mathfrak{P}}$, $V_{Y\mathfrak{P}}$ and $V_{X\mathfrak{Q}}$ are subspaces of $V_{X\mathfrak{P}}^*$, we deduce from Galerkin orthogonality, (4.2), (4.5) and (4.3b), that

$$B_0(e_0^*, v_{X\mathfrak{P}}) = 0 \qquad \forall\, v_{X\mathfrak{P}} \in V_{X\mathfrak{P}}, \tag{4.9}$$

$$B_0(e_0^*, v_{Y\mathfrak{P}}) = B_0(e_{Y\mathfrak{P}}, v_{Y\mathfrak{P}}) \qquad \forall\, v_{Y\mathfrak{P}} \in V_{Y\mathfrak{P}}, \tag{4.10}$$

$$B_0(e_0^*, v_{X\mathfrak{Q}}) = B_0(e_{X\mathfrak{Q}}, v_{X\mathfrak{Q}}) \qquad \forall\, v_{X\mathfrak{Q}} \in V_{X\mathfrak{Q}}. \tag{4.11}$$

Then using (4.11) with $v_{X\mathfrak{Q}} = e_{X\mathfrak{Q}}$ and (4.10) with $v_{Y\mathfrak{P}} = e_{Y\mathfrak{P}}$, we obtain

$$\begin{aligned} B_0(e_0^*, e_{Y\mathfrak{P}} + e_{X\mathfrak{Q}}) &= B_0(e_0^* - e_{X\mathfrak{Q}}, e_{Y\mathfrak{P}} + e_{X\mathfrak{Q}}) + B_0(e_{X\mathfrak{Q}}, e_{Y\mathfrak{P}} + e_{X\mathfrak{Q}}) \\ &= B_0(e_0^* - e_{X\mathfrak{Q}}, e_{Y\mathfrak{P}}) + B_0(e_{X\mathfrak{Q}}, e_{Y\mathfrak{P}} + e_{X\mathfrak{Q}}) \\ &= B_0(e_0^*, e_{Y\mathfrak{P}}) + B_0(e_{X\mathfrak{Q}}, e_{X\mathfrak{Q}}) \\ &= B_0(e_{Y\mathfrak{P}}, e_{Y\mathfrak{P}}) + B_0(e_{X\mathfrak{Q}}, e_{X\mathfrak{Q}}) = \eta^2. \end{aligned}$$

Hence, applying the Cauchy-Schwarz inequality and recalling the formula (4.7) for η, we establish the left-hand inequality in (4.8).

In order to prove the right-hand inequality in (4.8), we represent $e_0^* \in V_{X\mathfrak{P}}^*$ as

$$e_0^* = w_{X\mathfrak{P}} + w_{Y\mathfrak{P}} + w_{X\mathfrak{Q}}, \tag{4.12}$$

where $w_{X\mathfrak{P}} \in V_{X\mathfrak{P}}$, $w_{Y\mathfrak{P}} \in V_{Y\mathfrak{P}}$, and $w_{X\mathfrak{Q}} \in V_{X\mathfrak{Q}}$. Then, using (4.9)–(4.11) and then applying the discrete Cauchy–Schwarz inequality we obtain

$$\begin{aligned} \|e_0^*\|_{B_0}^2 &= B_0(e_0^*, w_{X\mathfrak{P}} + w_{Y\mathfrak{P}} + w_{X\mathfrak{Q}}) = B_0(e_{Y\mathfrak{P}}, w_{Y\mathfrak{P}}) + B_0(e_{X\mathfrak{Q}}, w_{X\mathfrak{Q}}) \\ &\le \|e_{Y\mathfrak{P}}\|_{B_0}\,\|w_{Y\mathfrak{P}}\|_{B_0} + \|e_{X\mathfrak{Q}}\|_{B_0}\,\|w_{X\mathfrak{Q}}\|_{B_0} \\ &\le \eta\left(\|w_{Y\mathfrak{P}}\|_{B_0}^2 + \|w_{X\mathfrak{Q}}\|_{B_0}^2\right)^{1/2}. \end{aligned} \tag{4.13}$$

On the other hand, using representation (4.12), the orthogonality (3.9) of polynomial spaces $\mathcal{P}_{\mathfrak{P}}$ and $\mathcal{P}_{\mathfrak{Q}}$ with respect to the measure π, and the strengthened Cauchy–Schwarz inequality (3.11), we can estimate

$$\begin{aligned}\|e_0^*\|_{B_0}^2 &= \|w_{X\mathfrak{P}}\|_{B_0}^2 + \|w_{Y\mathfrak{P}}\|_{B_0}^2 + \|w_{X\mathfrak{Q}}\|_{B_0}^2 + 2B_0(w_{X\mathfrak{P}}, w_{Y\mathfrak{P}}) \\ &\geq \|w_{X\mathfrak{P}}\|_{B_0}^2 + \|w_{Y\mathfrak{P}}\|_{B_0}^2 + \|w_{X\mathfrak{Q}}\|_{B_0}^2 - 2\gamma \|w_{X\mathfrak{P}}\|_{B_0} \|w_{Y\mathfrak{P}}\|_{B_0}. \\ &\geq (1-\gamma^2)\left(\|w_{Y\mathfrak{P}}\|_{B_0}^2 + \|w_{X\mathfrak{Q}}\|_{B_0}^2\right). \end{aligned} \tag{4.14}$$

The right-hand inequality in (4.8) then follows from (4.13) and (4.14). ∎

Remark 4.1. The error decomposition is subtle, for any $v_{X\mathfrak{Q}} \in V_{X\mathfrak{Q}}$ we have

$$B_0(e_{X\mathfrak{Q}} - w_{X\mathfrak{Q}}, v_{X\mathfrak{Q}}) \overset{(4.11)}{=} B_0(e_0^* - w_{X\mathfrak{Q}}, v_{X\mathfrak{Q}}) \overset{(4.12)}{=} B_0(w_{X\mathfrak{P}} + w_{Y\mathfrak{P}}, v_{X\mathfrak{Q}}) \overset{(3.9)}{=} 0,$$

showing that $w_{X\mathfrak{Q}} = e_{X\mathfrak{Q}}$. On the other hand, $w_{Y\mathfrak{P}} \neq e_{Y\mathfrak{P}}$, in general (here, the equality does hold when the subspaces X and Y in (3.6) are orthogonal with respect to the inner product $\langle A_0 \cdot, \cdot \rangle$). Therefore, $\|e_0^*\|_{B_0} \neq \eta$, in general, and the constant in the upper bound in (4.8) only depends on the constant γ that measures the angle between the subspaces X and Y (with respect to the inner product $\langle A_0 \cdot, \cdot \rangle$). Note that if X and Y are orthogonal then $\gamma = 0$ and (4.8) implies $\|e_0^*\|_{B_0} = \eta$.

Combining the results of Proposition 4.1 and Lemma 4.1 gives two-sided bounds for the energy error $\|e\|_B = \|u - u_{X\mathfrak{P}}\|_B$ in terms of the estimate η.

Theorem 4.1. *Let $u \in V$ be the solution to problem (2.2), and let $u_{X\mathfrak{P}} \in V_{X\mathfrak{P}}$ be the Galerkin approximation satisfying (3.5). Suppose that Assumption 3.1 holds. Then, the a posteriori error estimate η defined by (4.6) satisfies*

$$\sqrt{\lambda}\,\eta \leq \|u - u_{X\mathfrak{P}}\|_B \leq \frac{\sqrt{\Lambda}}{\sqrt{1-\beta^2}\,\sqrt{1-\gamma^2}}\,\eta, \tag{4.15}$$

where λ, Λ are the constants in (2.7), $\gamma \in [0,1)$ is the constant in the strengthened Cauchy–Schwarz inequality (3.7), and $\beta \in [0,1)$ is the constant in (3.15).

Remark 4.2. *We note the improved constant in the lower bound in (4.15) when compared to the corresponding error bound in the precursor paper* [4, Theorem 4.1].

Remark 4.3. *The error estimation strategy immediately extends to multilevel Galerkin approximations of (2.2). In particular, given finite-dimensional subspaces $X_\nu \subset H$ ($\nu \in \mathfrak{P}$), we can define the multilevel finite dimensional subspace of V as the space*

$$V_{X\mathfrak{P}} := \bigoplus_{\nu \in \mathfrak{P}} \left(X_\nu \otimes \mathcal{P}_\nu\right).$$

We can also construct an enriched subspace

$$V_{X\mathfrak{P}}^* := \underbrace{\Big(\bigoplus_{\nu \in \mathfrak{P}} \left(X_\nu^* \otimes \mathcal{P}_\nu\right)\Big)}_{V_{X\mathfrak{P}} \,\oplus\, V_{Y\mathfrak{P}}} \oplus \Big(\underbrace{X_{\bar\nu} \otimes \mathcal{P}_{\mathfrak{Q}}}_{V_{X\mathfrak{Q}}}\Big),$$

where X_ν^* ($\nu \in \mathfrak{P}$) are the enriched finite-dimensional subspaces of H such that $X_\nu^* = X_\nu \oplus Y_\nu$ with detail spaces $Y_\nu \subset H$. The detail index set $\mathfrak{Q} \subset \mathfrak{I}$ is such that $\mathfrak{P} \cap \mathfrak{Q} = \emptyset$, and $\bar\nu$ is any one of the indices in $\mathfrak{P}$ (e.g., $\bar\nu$ is such that $\dim(X_{\bar\nu}) = \max\{\dim(X_\nu);\, \nu \in \mathfrak{P}\}$). Theorem 4.1 remains valid if we define η as in (4.6) with $e_{Y\mathfrak{P}}$ and $e_{X\mathfrak{Q}}$ given by (4.5) and (4.3b), respectively. The only change is that the constant γ in (4.15) is now defined as $\gamma := \max\{\gamma_\nu;\, \nu \in \mathfrak{P}\}$, where γ_ν denotes the constant in the strengthened Cauchy–Schwarz inequality for the subspaces X_ν, $Y_\nu \subset H$.

4.1. Estimates of the error reduction. As discussed in [4, section 5], it turns out that the error estimates $\|e_{Y\mathfrak{P}}\|_{B_0}$ and $\|e_{X\mathfrak{Q}}\|_{B_0}$ contributing to η in (4.6) also provide effective estimates for the error reductions that would result if we were to compute the enhanced Galerkin approximations $u_{X^*\mathfrak{P}} \in V_{X^*\mathfrak{P}}$ and $u_{X\mathfrak{P}^*} \in V_{X\mathfrak{P}^*} := X \otimes \mathcal{P}_{\mathfrak{P}^*}$ by solving the discrete problems

$$B(u_{X^*\mathfrak{P}}, v) = F(v) \qquad \forall\, v \in V_{X^*\mathfrak{P}}, \tag{4.16a}$$

$$B(u_{X\mathfrak{P}^*}, v) = F(v) \qquad \forall\, v \in V_{X\mathfrak{P}^*}. \tag{4.16b}$$

We recall from [4, equation (5.3)] that in the case of the enhanced approximation $u_{X^*\mathfrak{P}}$ satisfying (4.16a), the Galerkin orthogonality property and the Pythagorean theorem yield the equality

$$\|e\|_B^2 = \|e_{X^*\mathfrak{P}}\|_B^2 + \|u_{X^*\mathfrak{P}} - u_{X\mathfrak{P}}\|_B^2, \tag{4.17}$$

where $e = u - u_{X\mathfrak{P}}$ and $e_{X^*\mathfrak{P}} = u - u_{X^*\mathfrak{P}}$. From (4.17) we conclude that the error reduction achieved by enriching only the subspace $X \subset H$ is characterized by the quantity $\|u_{X^*\mathfrak{P}} - u_{X\mathfrak{P}}\|_B$. In the same way, the error reduction achieved by enriching only the polynomial subspace $\mathcal{P}_{\mathfrak{P}}$ is characterized by the quantity $\|u_{X\mathfrak{P}^*} - u_{X\mathfrak{P}}\|_B$, where $u_{X\mathfrak{P}^*} \in V_{X\mathfrak{P}^*}$ solves (4.16b). The following theorem establishes two-sided bounds for both error reductions in terms of the estimates $\|e_{Y\mathfrak{P}}\|_{B_0}$ and $\|e_{X\mathfrak{Q}}\|_{B_0}$.

THEOREM 4.2. [4, Theorem 5.1] *Let $u_{X\mathfrak{P}} \in V_{X\mathfrak{P}}$ be the Galerkin approximation satisfying* (3.5)*, and let $u_{X^*\mathfrak{P}} \in V_{X^*\mathfrak{P}}$ and $u_{X\mathfrak{P}^*} \in V_{X\mathfrak{P}^*}$ be the enhanced approximations satisfying* (4.16)*. Then, there hold the following estimates for the error reduction*

$$\sqrt{\lambda}\,\|e_{Y\mathfrak{P}}\|_{B_0} \le \|u_{X^*\mathfrak{P}} - u_{X\mathfrak{P}}\|_B \le \frac{\sqrt{\Lambda}}{\sqrt{1-\gamma^2}}\,\|e_{Y\mathfrak{P}}\|_{B_0}, \tag{4.18}$$

$$\sqrt{\lambda}\,\|e_{X\mathfrak{Q}}\|_{B_0} \le \|u_{X\mathfrak{P}^*} - u_{X\mathfrak{P}}\|_B \le \sqrt{\Lambda}\,\|e_{X\mathfrak{Q}}\|_{B_0}, \tag{4.19}$$

where $e_{Y\mathfrak{P}} \in Y \otimes \mathcal{P}_{\mathfrak{P}}$ and $e_{X\mathfrak{Q}} \in X \otimes \mathcal{P}_{\mathfrak{Q}}$ are defined by (4.5) *and* (4.3b)*, λ, Λ are the constants in* (2.7)*, and $\gamma \in [0,1)$ is the constant appearing in the strengthened Cauchy–Schwarz inequality* (3.7)*.*

4.2. The error estimator $e_{X\mathfrak{Q}}$. The properties of the estimator $e_{X\mathfrak{Q}}$ play an important role in the implementation of our error estimation strategy. It goes without saying that the estimator $e_{X\mathfrak{Q}}$ depends on the choice of the detail index set $\mathfrak{Q}$, and, generally speaking, two detail index sets $\mathfrak{Q}_1, \mathfrak{Q}_2 \subset \mathfrak{I}$ result in different estimators $e^{(1)}_{X\mathfrak{Q}} \in V^{(1)}_{X\mathfrak{Q}}$ and $e^{(2)}_{X\mathfrak{Q}} \in V^{(2)}_{X\mathfrak{Q}}$ satisfying

$$B_0(e^{(i)}_{X\mathfrak{Q}}, v) = F(v) - B(u_{X\mathfrak{P}}, v) \quad \forall\, v \in V^{(i)}_{X\mathfrak{Q}}, \quad i = 1, 2, \tag{4.20}$$

respectively (where $V^{(i)}_{X\mathfrak{Q}} = X \otimes \mathcal{P}_{\mathfrak{Q}_i}$). The next lemma establishes a simple relation between these two error estimators and the error estimator $e_{X\mathfrak{Q}}$ corresponding to the combined index set $\mathfrak{Q} = \mathfrak{Q}_1 \cup \mathfrak{Q}_2$.

LEMMA 4.2. *Let $\mathfrak{Q}$, $\mathfrak{Q}_1$, $\mathfrak{Q}_2 \subset \mathfrak{I}$ be three detail index sets such that $\mathfrak{Q} = \mathfrak{Q}_1 \cup \mathfrak{Q}_2$ and $\mathfrak{Q}_1 \cap \mathfrak{Q}_2 = \emptyset$. If $e_{X\mathfrak{Q}}$, $e^{(1)}_{X\mathfrak{Q}}$, $e^{(2)}_{X\mathfrak{Q}}$ are the parameter error estimators corresponding to these index sets satisfying* (4.3b) *and* (4.20) *then*

$$e_{X\mathfrak{Q}} = e^{(1)}_{X\mathfrak{Q}} + e^{(2)}_{X\mathfrak{Q}} \quad \textit{and} \quad \big\|e_{X\mathfrak{Q}}\big\|^2_{B_0} = \big\|e^{(1)}_{X\mathfrak{Q}}\big\|^2_{B_0} + \big\|e^{(2)}_{X\mathfrak{Q}}\big\|^2_{B_0}. \tag{4.21}$$

Proof. For any $v \in V_{X\mathfrak{Q}}^{(i)} = X \otimes \mathcal{P}_{\mathfrak{Q}_i}$, $i = 1, 2$, we have the representation

$$v(\mathbf{y}) = \sum_{\mu \in \mathfrak{Q}_i} \psi_\mu P_\mu(\mathbf{y}) \quad \text{with } \psi_\mu \in X.$$

(Note that ψ_μ is a function of $\mathbf{x}$ in a PDE setting, in which case v is also a function of $\mathbf{x}$.) Similarly, for $e_{X\mathfrak{Q}} \in V_{X\mathfrak{Q}} = X \otimes \mathcal{P}_{\mathfrak{Q}} = X \otimes \big(\mathcal{P}_{\mathfrak{Q}_1} \oplus \mathcal{P}_{\mathfrak{Q}_2}\big)$, we write

$$e_{X\mathfrak{Q}}(\mathbf{y}) = \sum_{\nu \in \mathfrak{Q}} \phi_\nu P_\nu(\mathbf{y}) = \Big(\sum_{\nu \in \mathfrak{Q}_1} + \sum_{\nu \in \mathfrak{Q}_2} \Big) \phi_\nu P_\nu(\mathbf{y}) =: w_1(\mathbf{y}) + w_2(\mathbf{y})$$

with $\phi_\nu \in X$ and $w_i \in V_{X\mathfrak{Q}}^{(i)}$, $i = 1, 2$. Using this decomposition, (4.3b) takes the form

$$B_0(w_1, v) + B_0(w_2, v) = F(v) - B(u_{X\mathfrak{P}}, v) \quad \forall\, v \in V_{X\mathfrak{Q}}. \tag{4.22}$$

Next, choosing $v \in V_{X\mathfrak{Q}}^{(1)} \subset V_{X\mathfrak{Q}}$,

$$\begin{aligned} B_0(w_2, v) &= \int_\Gamma \Big\langle A_0 \sum_{\nu \in \mathfrak{Q}_2} \phi_\nu\, P_\nu(\mathbf{y}),\, \sum_{\mu \in \mathfrak{Q}_1} \psi_\mu\, P_\mu(\mathbf{y}) \Big\rangle \, \mathrm{d}\pi(\mathbf{y}) \\ &= \sum_{\nu \in \mathfrak{Q}_2} \sum_{\mu \in \mathfrak{Q}_1} \langle A_0 \phi_\nu,\, \psi_\mu \rangle \int_\Gamma P_\nu(\mathbf{y})\, P_\mu(\mathbf{y})\, \mathrm{d}\pi(\mathbf{y}) = 0, \end{aligned} \tag{4.23}$$

because $\{P_\mu\}_{\mu \in \mathfrak{I}}$ is an orthonormal basis and $\mathfrak{Q}_1 \cap \mathfrak{Q}_2 = \emptyset$. Hence, from (4.22) we conclude that $w_1 \in V_{X\mathfrak{Q}}^{(1)}$ satisfies $B_0(w_1, v) = F(v) - B(u_{X\mathfrak{P}}, v)$, $\forall\, v \in V_{X\mathfrak{Q}}^{(1)}$. This is the same equation as (4.20) (with $i = 1$), and since (4.20) uniquely defines $e_{X\mathfrak{Q}}^{(1)}$, we deduce that $w_1 = e_{X\mathfrak{Q}}^{(1)}$. Testing with $v \in V_{X\mathfrak{Q}}^{(2)}$ in (4.22) we similarly deduce that $w_2 = e_{X\mathfrak{Q}}^{(2)}$. Therefore, $e_{X\mathfrak{Q}} = e_{X\mathfrak{Q}}^{(1)} + e_{X\mathfrak{Q}}^{(2)}$. The second equality in (4.21) immediately follows from (4.23). ∎

Given any finite detail set $\mathfrak{Q} = \{\mu \in \mathfrak{I}; \mu \notin \mathfrak{P}\}$, a consequence of Lemma 4.2 is that the associated error estimator $e_{X\mathfrak{Q}}$ can be decomposed into contributions from the estimators that correspond to individual indices $\mu \in \mathfrak{Q}$:

$$e_{X\mathfrak{Q}} = \sum_{\mu \in \mathfrak{Q}} e_{X\mathfrak{Q}}^{(\mu)} \quad \text{with} \quad \|e_{X\mathfrak{Q}}\|_{B_0}^2 = \sum_{\mu \in \mathfrak{Q}} \big\|e_{X\mathfrak{Q}}^{(\mu)}\big\|_{B_0}^2, \tag{4.24}$$

where $e_{X\mathfrak{Q}}^{(\mu)} \in X \otimes \mathcal{P}_\mu$ satisfies

$$B_0\big(e_{X\mathfrak{Q}}^{(\mu)}, v\big) = F(v) - B(u_{X\mathfrak{P}}, v) \qquad \forall\, v \in X \otimes \mathcal{P}_\mu. \tag{4.25}$$

Each estimator $e_{X\mathfrak{Q}}^{(\mu)}$ can be independently and cheaply computed (in fact, the linear systems associated with (4.25) for all $\mu \in \mathfrak{Q}$ have the same coefficient matrix, see section 5). A second key point is that, thanks to Theorem 4.2, the norm $\big\|e_{X\mathfrak{Q}}^{(\mu)}\big\|_{B_0}$ provides an estimate for the error reduction that would be achieved by including the individual index μ in the enriched index set $\mathfrak{P}^*$ and computing the corresponding enhanced approximation $u_{X\mathfrak{P}^*}$.

An equally important aspect of the construction of an efficient adaptive refinement algorithm is the need to account for the large number of indices $\mu \in \mathfrak{I} \backslash \mathfrak{P}$ for which the

error estimator $e_{X\mathfrak{Q}}^{(\mu)}$, and hence the corresponding error reduction, is equal to zero. Some notation is needed first: for any $m \in \mathbb{N}$, we let $\varepsilon^{(m)} = \left(\varepsilon_1^{(m)}, \varepsilon_2^{(m)}, \dots\right) \in \mathfrak{I}$ represent the Kronecker delta sequence for the coordinate m, i.e., $\varepsilon_j^{(m)} = \delta_{jm}$ for any $j \in \mathbb{N}$. Then, for any finite index set $\mathfrak{P}$ we define $\mathfrak{P}_\infty^*$ to be the infinite index set given by $\mathfrak{P}_\infty^* := \mathfrak{P} \cup \mathfrak{Q}_\infty$, where

$$\mathfrak{Q}_\infty := \left\{ \mu \in \mathfrak{I} \setminus \mathfrak{P};\ \mu = \nu \pm \varepsilon^{(m)},\ \forall \nu \in \mathfrak{P},\ \forall m = 1, 2, \dots \right\}. \tag{4.26}$$

The nonzero contributions to the error estimator $e_{X\mathfrak{Q}}$ are associated with the boundary of the current index set. We identify the corresponding indices in the following lemma.

LEMMA 4.3. *Assume that the detail index set $\mathfrak{Q}$ is a finite subset of the index set $\mathfrak{I} \setminus \mathfrak{P}_\infty^*$ and let $f : \Gamma \to H'$ be the parametric linear functional in* (2.1)*. The associated estimator $e_{X\mathfrak{Q}}$ is equal to zero if and only if*

$$F(v) = \int_\Gamma \langle f(\mathbf{y}), v(\mathbf{y}) \rangle \, d\pi(\mathbf{y}) = 0 \quad \forall\, v \in V_{X\mathfrak{Q}}. \tag{4.27}$$

Proof. Thanks to Lemma 4.2, it is sufficient to consider the detail index set $\mathfrak{Q}$ comprising a single index, that is $\mathfrak{Q} = \{\mu\}$, where $\mu \notin \mathfrak{P}_\infty^*$. The key step is to show that the error estimator $e_{X\mathfrak{Q}} \in V_{X\mathfrak{Q}} = X \otimes \mathcal{P}_\mu$ satisfies $B_0(e_{X\mathfrak{Q}}, v) = F(v)$, $\forall\, v \in V_{X\mathfrak{Q}}$. Then, since $B_0(\cdot, \cdot)$ generates a norm on V, the result is an immediate consequence of (4.27). Thus, using the error equation (4.3b) we simply need to show that for arbitrary $v \in V_{X\mathfrak{Q}}$ we have

$$F(v) - B_0(e_{X\mathfrak{Q}}, v) = B(u_{X\mathfrak{P}}, v) = B_0(u_{X\mathfrak{P}}, v) + \sum_{m=1}^{\infty} B_m(u_{X\mathfrak{P}}, v) = 0. \tag{4.28}$$

To establish (4.28), recall that $u_{X\mathfrak{P}}(\mathbf{y}) = \sum_{\nu \in \mathfrak{P}} \phi_\nu \, P_\nu(\mathbf{y}) \in V_{X\mathfrak{P}}$ with $\phi_\nu \in X$ and $v(\mathbf{y}) = \phi_\mu \, P_\mu(\mathbf{y}) \in V_{X\mathfrak{Q}}$ with $\phi_\mu \in X$. First, since $\mu \notin \mathfrak{P}$, we get

$$\begin{aligned} B_0(u_{X\mathfrak{P}}, v) &= \int_\Gamma \langle A_0 u_{X\mathfrak{P}}(\mathbf{y}), v(\mathbf{y}) \rangle d\pi(\mathbf{y}) \\ &= \sum_{\nu \in \mathfrak{P}} \langle A_0 \phi_\nu, \phi_\mu \rangle \int_\Gamma P_\nu(\mathbf{y}) P_\mu(\mathbf{y}) d\pi(\mathbf{y}) = 0. \end{aligned}$$

Next, for any fixed $m = 1, 2, \dots$, we get

$$\begin{aligned} B_m(u_{X\mathfrak{P}}, v) &= \int_\Gamma \langle A_m u_{X\mathfrak{P}}(\mathbf{y}), v(\mathbf{y}) \rangle \, y_m d\pi(\mathbf{y}) \\ &= \sum_{\nu \in \mathfrak{P}} \langle A_m \phi_\nu, \phi_\mu \rangle \int_\Gamma P_\nu(\mathbf{y}) P_\mu(\mathbf{y}) y_m d\pi(\mathbf{y}) = 0 \end{aligned}$$

thanks to the three-term recurrence (3.2) and the fact that $\mu \notin \mathfrak{P}_\infty^*$. ∎

We now show that (4.27) holds in the important case when the parametric linear functional $f(\mathbf{y})$ has affine dependence on the parameters y_m (and in particular, when f is parameter free as in our model problem (2.8)).

COROLLARY 4.1. *Assume that $f(\mathbf{y})$ has the decomposition*

$$f(\mathbf{y}) = f_0 + \sum_{m=1}^{\infty} y_m f_m, \quad \forall\, \mathbf{y} \in \Gamma \tag{4.29}$$

with $f_m \in H'$ ($m \in \mathbb{N}_0$) and convergence of the series to be understood in H' uniformly in $\mathbf{y}$. Let the detail index set $\mathfrak{Q}$ be any finite subset of the index set $\mathfrak{I} \setminus \mathfrak{P}^*_\infty$. Then the corresponding estimator $e_{X\mathfrak{Q}}$ is equal to zero.

Proof. The assertion will follow by Lemma 4.3 if we prove that $F(v) = 0$ for any $v \in V_{X\mathfrak{Q}}$. It is again sufficient to consider $\mathfrak{Q} = \{\mu\}$ with some $\mu \notin \mathfrak{P}^*_\infty$. In this case, for any $v(\mathbf{y}) = \phi_\mu\, P_\mu(\mathbf{y}) \in V_{X\mathfrak{Q}}$ one has

$$F(v) = \langle f_0, \phi_\mu \rangle \int_\Gamma P_\mu(\mathbf{y}) d\pi(\mathbf{y}) + \sum_{m=1}^{\infty} \langle f_m, \phi_\mu \rangle \int_\Gamma y_m P_\mu(\mathbf{y}) d\pi(\mathbf{y}).$$

Here, $\int_\Gamma P_\mu(\mathbf{y}) d\pi(\mathbf{y}) = 0$ because $\mu \neq \mathbf{0}$ (recall that $\mathbf{0} \in \mathfrak{P}$), and $\int_\Gamma y_m P_\mu(\mathbf{y}) d\pi(\mathbf{y}) = 0$ for all $m \in \mathbb{N}$ due to the three-term recurrence (3.2) and because $\mu \neq \varepsilon^{(m)}$ for any $m \in \mathbb{N}$ (note that $\varepsilon^{(m)} \in \mathfrak{P}^*_\infty$). Hence $F(v) = 0$. ∎

The enrichment of the polynomial space $\mathcal{P}_\mathfrak{P}$ on Γ is linked to the choice of the detail index set $\mathfrak{Q}$, for which the contributing estimator $e_{X\mathfrak{Q}}$ is computed. Lemma 4.3 and Corollary 4.1 suggest that even in the case of highly enriched polynomial spaces $\mathcal{P}_{\mathfrak{P}\cup\mathfrak{Q}}$, the number of individual indices for which non-zero contributions $e^{(\mu)}_{X\mathfrak{Q}}$ need to be computed may actually be very few. We will illustrate this assertion with a simple example. Given integers $M \geq 1$ and $p \geq 0$ we denote by $\mathcal{P}_{M,p}$ the space of polynomials of total degree $\leq p$ in the first M parameters y_m, $m = 1, \ldots, M$. Note that $\mathcal{P}_{M,p}$ can be equivalently defined as the span of the tensorized Legendre polynomials $P_\nu(\mathbf{y})$ so that

$$\nu \in \mathfrak{P}_{M,p} := \Big\{ \nu = (\nu_1, \nu_2, \ldots) \in \mathbb{N}_0^{\mathbb{N}};\ \operatorname{supp} \nu \subset \{1, \ldots, M\},\ \textstyle\sum_{m=1}^{M} \nu_m \leq p \Big\}.$$

The dimension of $\mathcal{P}_{M,p}$ is given by $\dim(\mathcal{P}_{M,p}) = \#(\mathfrak{P}_{M,p}) = \frac{(p+M)!}{p!\,M!}$.

EXAMPLE 4.1. *Fix the polynomial space on Γ to be $\mathcal{P}_{3,2}$ and consider an enriched polynomial space $\mathcal{P}_{10,5} = \mathcal{P}_{3,2} \oplus \mathcal{P}_\mathfrak{Q}$ with detail index set $\mathfrak{Q} = \mathfrak{P}_{10,5} \setminus \mathfrak{P}_{3,2}$. Then* $\dim(\mathcal{P}_\mathfrak{Q}) = \dim(\mathcal{P}_{10,5}) - \dim(\mathcal{P}_{3,2}) = 2993$. *However, from the result in Lemma 4.3, the number of indices $\mu \in \mathfrak{Q}$ associated with nonzero refinement estimators $e^{(\mu)}_{X\mathfrak{Q}}$ (i.e., that need to be computed) is only*

$$\#(\mathfrak{Q} \cap \mathfrak{Q}_\infty) = \big(\dim(\mathcal{P}_{3,3}) - \dim(\mathcal{P}_{3,2})\big) + (10-3) \cdot \dim(\mathcal{P}_{3,2}) = 80\,(!)$$

The above discussion indicates that if the error estimation strategy is to be effective, then the detail index set $\mathfrak{Q}$ should be a sufficiently large (finite) subset of the index set $\mathfrak{Q}_\infty$. This conclusion underpins the specific choice of $\mathfrak{Q}$ in the adaptive algorithm presented in the next section.

5. Adaptive algorithm. A generic adaptive refinement algorithm is discussed in this section. Its efficiency is a consequence of the theoretical results of the previous section. To fix notation, the algorithmic components are developed in the context of the model diffusion problem (2.8) with a random coefficient $a = a(\mathbf{x}, \mathbf{y})$ represented by the parametric form (2.9). The extension of the algorithm to other parametric operator equations will be immediately obvious.

The variational formulation of (2.8) is given by (2.2)–(2.3) where the parametric operator $A(\mathbf{y})$ is defined by (2.11) for all $\mathbf{y} \in \Gamma$, $f \in H^{-1}(D)$, and $V := L^2_\pi(\Gamma, H^1_0(D))$. We will construct a finite-dimensional subspace of V by tensorizing standard finite element functions of $\mathbf{x} \in D$ and multivariate polynomials of $\mathbf{y} \in \Gamma$. Our finite element

approximation will be conforming: for example, piecewise bilinear or biquadratic approximation on shape-regular partition Δ_h of D. (Here, $h > 0$ denotes the length of the longest element edge in the resulting mesh). We will denote the associated finite element space by $X(h)$. Next, given a finite index set $\mathfrak{P} \subset \mathfrak{I}$ (this is built adaptively by the algorithm), we take the finite-dimensional subspace $\mathcal{P}_{\mathfrak{P}}$ of $L^2_\pi(\Gamma)$ described in section 3. The resulting finite-dimensional subspace of V is $V_N = V_{X\mathfrak{P}} := X(h) \otimes \mathcal{P}_{\mathfrak{P}}$. Here, $N = N(h, \mathfrak{P})$ denotes the total number of degrees of freedom, and is simply the product of the number of spatial degrees of freedom and the cardinality of $\mathfrak{P}$. The stochastic Galerkin finite element (sGFEM) solution $u_{X\mathfrak{P}} \in V_{X\mathfrak{P}}$ is uniquely defined by the identity (3.5).

To control the error in the Galerkin approximation, we compute the energy estimate η defined by (4.6) and stop the adaptive process when a prescribed tolerance, *tol*, is satisfied. To compute the component estimators $e_{Y\mathfrak{P}}$ and $e_{X\mathfrak{Q}}$ that contribute to η, the construction of the detail spaces on D and Γ need to be explicitly specified. In our algorithm, $Y(h)$ will be local bubble functions: these can either be defined by higher order polynomials (for example, biquartic in the case of a biquadratic space $X(h)$ or biquadratic in the case of a bilinear space $X(h)$) or else by constructing piecewise polynomials (biquadratic or bilinear) on a refined mesh $\Delta_{h/2}$. The detail polynomial space $\mathcal{P}_{\mathfrak{Q}}$ is associated with the following index set (cf. (4.26))

$$\mathfrak{Q} = \left\{ \mu \in \mathfrak{I} \setminus \mathfrak{P};\ \mu = \nu \pm \varepsilon^{(m)},\ \forall \nu \in \mathfrak{P},\ \forall m = 1, 2, \ldots, M_{\mathfrak{P}} + 1 \right\}, \tag{5.1}$$

where the parameter counter $M_{\mathfrak{P}}$ is defined as follows

$$M_{\mathfrak{P}} := \begin{cases} 0 & \text{if } \mathfrak{P} = \{\mathbf{0}\}, \\ \max\left\{ \max(\operatorname{supp} \nu);\ \nu \in \mathfrak{P} \setminus \{\mathbf{0}\} \right\} & \text{otherwise.} \end{cases} \tag{5.2}$$

The error estimators $e_{Y\mathfrak{P}}$ and $e_{X\mathfrak{Q}}$ satisfy the discrete formulations (4.5) and (4.3b) with $V_{Y\mathfrak{P}} := Y(h) \otimes \mathcal{P}_{\mathfrak{P}}$, $V_{X\mathfrak{Q}} := X(h) \otimes \mathcal{P}_{\mathfrak{Q}}$, and with the bilinear form $B_0(\cdot, \cdot)$ (cf. (2.6), (2.12)) defined by $B_0(v, w) = \int_\Gamma \int_D a_0(\mathbf{x}) \nabla v(\mathbf{x}, \mathbf{y}) \cdot \nabla w(\mathbf{x}, \mathbf{y}) \, \mathrm{d}\mathbf{x} \, \mathrm{d}\pi(\mathbf{y})$. The spatial error estimator $e_{Y\mathfrak{P}}$ is computed using the strategy described in the precursor paper [4]. On each element $K \in \Delta_h$ we use a standard element residual technique (see, e.g., Ainsworth & Oden [1]) to construct the following local residual problem corresponding to (4.5): find $e_{Y\mathfrak{P}}|_K \in Y(h)|_K \otimes \mathcal{P}_{\mathfrak{P}}$ satisfying

$$\begin{aligned} B_{0,K}(e_{Y\mathfrak{P}}|_K, v) = F_K(v) &+ \int_\Gamma \int_K \nabla \cdot \left(a(\mathbf{x}, \mathbf{y}) \nabla u_{X\mathfrak{P}}(\mathbf{x}, \mathbf{y}) \right) v(\mathbf{x}, \mathbf{y}) \, \mathrm{d}\mathbf{x} \, \mathrm{d}\pi(\mathbf{y}) \\ &- \frac{1}{2} \int_\Gamma \int_{\partial K \setminus \partial D} a(s, \mathbf{y}) \left[\!\!\left[\frac{\partial u_{X\mathfrak{P}}}{\partial n} \right]\!\!\right] v(s, \mathbf{y}) \, \mathrm{d}s \, \mathrm{d}\pi(\mathbf{y}), \end{aligned} \tag{5.3}$$

for any $v \in Y(h)|_K \otimes \mathcal{P}_{\mathfrak{P}}$. Here, $B_{0,K}(\cdot, \cdot)$ and $F_K(\cdot)$ are the elementwise bilinear form and linear functional, respectively, $Y(h)|_K$ is the restriction of the finite element detail space to the element K, and $\left[\!\!\left[\frac{\partial u_{X\mathfrak{P}}}{\partial n} \right]\!\!\right]$ denotes the flux jump in the approximate solution $u_{X\mathfrak{P}}$ across inter-element edges. We refer to [4] for details of the linear algebra associated with solving (5.3).

The parameter error estimator $e_{X\mathfrak{Q}}$ is computed by combining the contributing estimators $e^{(\mu)}_{X\mathfrak{Q}}$ corresponding to individual indices $\mu \in \mathfrak{Q}$ (see (4.24)). Each contributing estimator $e^{(\mu)}_{X\mathfrak{Q}} \in X(h) \otimes \mathcal{P}_\mu$ is computed by solving the linear system associated with discrete formulation (4.25). The coefficient matrix of this linear system

represents the assembled stiffness matrix corresponding to the parameter-free term $a_0(x)$ (see (2.9)) on Δ_h, and is therefore the same for all $\mu \in \mathfrak{Q}$. Once the stiffness matrix has been factorized, the estimators $e^{(\mu)}_{X\mathfrak{Q}}$ can be computed independently by using forward and backward substitutions. Once all contributing estimators $e_{Y\mathfrak{P}}$ and $e^{(\mu)}_{X\mathfrak{Q}}$ ($\mu \in \mathfrak{Q}$) have been computed, the total error estimate η can be calculated via

$$\eta = \left(\|e_{Y\mathfrak{P}}\|^2_{B_0} + \sum_{\mu\in\mathfrak{Q}} \left\|e^{(\mu)}_{X\mathfrak{Q}}\right\|^2_{B_0} \right)^{1/2}. \tag{5.4}$$

If η exceeds the tolerance, we must enrich the subspace $V_{X\mathfrak{P}} = X(h) \otimes \mathcal{P}_{\mathfrak{P}}$ in order to compute a more accurate approximation. A key feature of our algorithm is that the estimators $e_{Y\mathfrak{P}}$ and $e^{(\mu)}_{X\mathfrak{Q}}$ ($\mu \in \mathfrak{Q}$) are individually probed in order to decide *how* to enrich the subspace $V_{X\mathfrak{P}}$. The motivation for this is that $\|e_{Y\mathfrak{P}}\|_{B_0}$ and $\|e^{(\mu)}_{X\mathfrak{Q}}\|_{B_0}$ provide effective estimates for the error reductions $\|u_{X^*\mathfrak{P}} - u_{X\mathfrak{P}}\|_B$ and $\|u_{X\mathfrak{P}^*} - u_{X\mathfrak{P}}\|_B$, respectively, where $u_{X^*\mathfrak{P}} \in V_{X^*\mathfrak{P}} = (X(h) \oplus Y(h)) \otimes \mathcal{P}_{\mathfrak{P}}$ and $u_{X\mathfrak{P}^*} \in V_{X\mathfrak{P}^*} = X(h) \otimes (\mathcal{P}_{\mathfrak{P}} \oplus \mathcal{P}_{\mu})$. Therefore, the dominant estimate indicates which part of the approximation space $V_{X\mathfrak{P}}$ ought to be enriched: either the finite element space on D or the polynomial space on Γ. In the former case, the enrichment is based on a global refinement of the spatial mesh Δ_h (typically, $\Delta_h \to \Delta_{h/2}$), whereas in the latter case, new indices are added to the index set $\mathfrak{P}$.

Algorithmically, this procedure is implemented as follows. We start with an initial finite element space $X(h_0)$, associated with a coarse mesh Δ_{h_0}, and an initial index set $\mathfrak{P}_0$ (e.g., $\mathfrak{P}_0 = \{(0,0,0,\ldots)\}$ or $\mathfrak{P}_0 = \{(0,0,0,\ldots),\ (1,0,0,\ldots)\}$). The goal of the algorithm is to generate a sequence of finite element spaces

$$X(h_0) \subset X(h_1) \subset X(h_2) \subset \ldots \subset X(h_n) \subset H^1_0(D)$$

(where h_{k+1} could be the same as h_k), and a sequence of index sets

$$\mathfrak{P}_0 \subset \mathfrak{P}_1 \subset \mathfrak{P}_2 \subset \ldots \subset \mathfrak{P}_n \subset \mathfrak{I}$$

such that the tolerance *tol* is met by the Galerkin solution $u_n \in X(h_n) \otimes \mathcal{P}_{\mathfrak{P}_n}$. At each step k, the Galerkin solution $u_{X\mathfrak{P}}$ and the error estimators $e_{Y\mathfrak{P}}$ and $e^{(\mu)}_{X\mathfrak{Q}}$ ($\mu \in \mathfrak{Q}$) are computed as described above. Then we find the maximum among the error estimates:

$$\delta := \max\left\{ \|e_{Y\mathfrak{P}}\|_{B_0};\ \max\left\{ \left\|e^{(\mu)}_{X\mathfrak{Q}}\right\|_{B_0};\ \mu \in \mathfrak{Q} \right\} \right\}.$$

If $\delta = \|e_{Y\mathfrak{P}}\|_{B_0}$, then the polynomial space on Γ is unchanged and the finite element space $X(h_k)$ is enriched. In our global refinement setting the enriched space $X(h_{k+1})$ is defined on a uniformly refined mesh: expressed in a hierarchical basis it is given by $X(h_k) \oplus Z(h_{k+1})$, where $Z(h_{k+1})$ is the span of Lagrangian basis functions defined at the newly introduced nodes. Otherwise, (if $\delta > \|e_{Y\mathfrak{P}}\|_{B_0}$) the finite element space is unchanged and the polynomial space on Γ is enriched by updating the index set (specifically, by including additional indices $\mu \in \mathfrak{Q}$ for which $\left\|e^{(\mu)}_{X\mathfrak{Q}}\right\|_{B_0} \geq \|e_{Y\mathfrak{P}}\|_{B_0}$). In this latter case, we set

$$\mathfrak{P}_{k+1} := \mathfrak{P}_k \cup \left\{ \mu \in \mathfrak{Q};\ \|e^{(\mu)}_{X\mathfrak{Q}}\|_{B_0} \geq \|e_{Y\mathfrak{P}}\|_{B_0} \right\},$$

so that $\mathcal{P}_{\mathfrak{P}_{n+1}} = \mathrm{span}\{P_\nu;\ \nu \in \mathfrak{P}_{n+1}\}$. The updated subspace $V_{X\mathfrak{P}} := X(h_{k+1}) \otimes \mathcal{P}_{\mathfrak{P}_{k+1}}$ can then be generated and a more accurate Galerkin solution can be computed. The process is then repeated until the tolerance is met.

ALGORITHM 5.1. `Adaptive_sGFEM` $[tol, A, f] \to u_n$
input $h_0,\ \mathfrak{P}_0$
for $k = 0, 1, 2, \ldots$ **do**
$u_k \leftarrow$ `Solve` $[A, f, X(h_k), \mathfrak{P}_k]$
$\delta_X \leftarrow$ `Error_Estimate_1` $[A, f, u_k, Y(h_k)]$
$\mathfrak{Q}_k \leftarrow$ `Detail_Index_Set` $[\mathfrak{P}_k]$
for $i = 1, 2, \ldots, \#(\mathfrak{Q}_k)$ **do**
$\delta_{\mathfrak{P},i} \leftarrow$ `Error_Estimate_2` $[A, f, u_k, \mu_i]$
end
$\eta_k := \left(\delta_X^2 + \sum_{i=1}^{\#(\mathfrak{Q}_k)} \delta_{\mathfrak{P},i}^2\right)^{1/2}$
if $\eta_k < tol$ **then** $n := k$**, break**
if $\delta_X \geq \max\left\{\delta_{\mathfrak{P},i};\ i = 1, 2, \ldots, \#(\mathfrak{Q}_k)\right\}$ **then**
$X(h_{k+1}) := X(h_k) \oplus Z(h_{k+1}),\ \ \mathfrak{P}_{k+1} := \mathfrak{P}_k$
else $X(h_{k+1}) := X(h_k),\ \ \mathfrak{P}_{k+1} := \mathfrak{P}_k \cup \left\{\mu_i \in \mathfrak{Q}_k;\ \delta_{\mathfrak{P},i} \geq \delta_X\right\}$
end

The complete algorithm is listed in Algorithm 5.1. A software implementation requires four functional building blocks:

- `Solve`$[A, f, X(h), \mathfrak{P}]$ — a subroutine that generates the Galerkin approximation $u_{X\mathfrak{P}} \in X(h) \otimes \mathcal{P}_{\mathfrak{P}}$ satisfying (3.5);
- `Detail_Index_Set`$[\mathfrak{P}]$ — a subroutine that generates the detailed index set $\mathfrak{Q}$ for the given index set $\mathfrak{P}$ (see (5.1));
- `Error_Estimate_1`$[A, f, u_{X\mathfrak{P}}, Y(h)]$ — a subroutine that computes the contributing error estimate based on X-enrichment (see the first term on the right-hand side of (4.6));
- `Error_Estimate_2`$[A, f, u_{X\mathfrak{P}}, \mu]$ — a subroutine that computes the contributing error estimate based on $\mathfrak{P}$-enrichment by a single index $\mu \notin \mathfrak{P}$ (see the second term on the right-hand side of (4.6) with $\mathfrak{Q} = \{\mu\}$).

The effectiveness of the adaptive strategy will be demonstrated by the numerical results that are presented in the next section.

6. Numerical experiments. Staying within the context of the two-dimensional diffusion problem (2.8) with the random coefficient $a = a(\mathbf{x}, \mathbf{y})$ in the parametric form (2.9), we follow Eigel et al. [7, Section 11] and select the expansion coefficients a_m, $m \in \mathbb{N}_0$ in (2.9) to represent planar Fourier modes of increasing total order. More precisely, we set $a_0(\mathbf{x}) := 1$ and

$$a_m(\mathbf{x}) := \alpha_m \cos(2\pi\beta_1(m)\, x_1) \cos(2\pi\beta_2(m)\, x_2),\ \ \mathbf{x} = (x_1, x_2) \in (0,1) \times (0,1). \quad (6.1)$$

The modes are ordered so that for any $m \in \mathbb{N}$,

$$\beta_1(m) = m - k(m)(k(m)+1)/2 \ \text{ and } \ \beta_2(m) = k(m) - \beta_1(m)$$

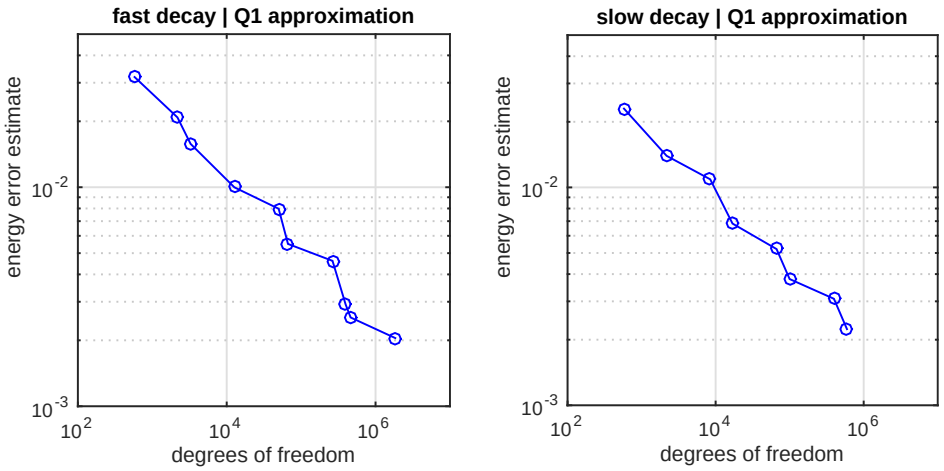

FIG. 6.1. *Error estimates at each step of the adaptive algorithm using Q_1 spatial approximation, with fast ($\tilde{\sigma} = 4$) and slow ($\tilde{\sigma} = 2$) decay of the amplitude coefficients.*

with $k(m) = \lfloor -1/2 + \sqrt{1/4 + 2m} \rfloor$, and the amplitude coefficients are constructed so that $\alpha_m = \bar{\alpha} m^{-\tilde{\sigma}}$ for fixed $\tilde{\sigma} > 1$ and $0 < \bar{\alpha} < 1/\zeta(\tilde{\sigma})$, where ζ denotes the Riemann zeta function. Note that for the coefficients given by (6.1), the inequalities in (2.13) and (2.14) hold with $\alpha_0^{\min} = \alpha_0^{\max} = 1$ and $\tau = \bar{\alpha}\zeta(\tilde{\sigma})$. Therefore, the variational formulation of (2.8) admits a unique solution $u \in V$.

In our numerical experiments we set $f(\mathbf{x}) = 1$. We consider expansions (2.9) with slow ($\tilde{\sigma} = 2$) and fast ($\tilde{\sigma} = 4$) decay of the amplitudes α_m in (6.1). In each case, we choose $\bar{\alpha}$ such that $\tau = \bar{\alpha}\zeta(\tilde{\sigma}) = 0.9$, which results in $\bar{\alpha} \approx 0.547$ for $\tilde{\sigma} = 2$ and $\bar{\alpha} \approx 0.832$ for $\tilde{\sigma} = 4$. We also assume that the parameters y_m in (2.9) are the images of uniformly distributed independent mean-zero random variables, and so $\pi_m = \pi_m(y_m)$ is the associated probability measure on $\Gamma_m = [-1, 1]$. This assumption ensures (2.10). The two problems are the same as those solved in [7, Section 11.1.1].

The performance of our adaptive algorithm was tested and numerical results will be presented for bilinear (Q_1) and biquadratic (Q_2) spatial approximation on uniform grids $\square_h$ of square elements of edge length h. The detail space $Y(h)$ (used in Algorithm 5.1 to compute the spatial error estimate δ_X) is defined differently in the two cases. For bilinear approximation, $Y(h)$ is simply the span of the set of bilinear bubble functions corresponding to edge midpoints and element centroids of the grid (this strategy is taken from the precursor paper [4, section 6.2]). For biquadratic approximation, $Y(h)$ spans a carefully selected set of biquartic bubble functions defined on $\square_h$. An assessment of the effectivity of this choice of detail space can be found in Liao [16, section 2.3].

The adaptive computation is initialized using an approximation space of fixed dimension. More precisely, in both the Q_1 and Q_2 cases we tensorize a coarse polynomial space $\mathcal{P}_{\mathfrak{P}_0}$ on Γ based on the initial index set

$$\mathfrak{P}_0 = \{(0, 0, 0, \ldots),\ (1, 0, 0, \ldots)\}$$

with a finite element space $X(h_0)$ associated with the coarse mesh $\square_{h_0}$, where $h_0 = 2^{-4}$ in the case of Q_1 approximation and $h_0 = 2^{-3}$ in the case of Q_2 approximation. When the finite element space $X(h)$ needs to be enriched within the adaptive algo-

rithm, this enrichment (for both Q_1 and Q_2 approximation) is based on a uniform refinement of the spatial mesh $\square_h$ (that is $\square_h \to \square_{h/2}$).

TABLE 6.1

Evolution of the index set at each step k of the adaptive algorithm using Q_1 approximation for fast ($\tilde{\sigma} = 4$) and slow ($\tilde{\sigma} = 2$) decay of the amplitude coefficients α_m. The entries '—' represent steps when a spatial refinement is performed.

k	fast decay	slow decay
0	(0 0)	(0 0 0 0)
	(1 0)	(1 0 0 0)
1	—	—
2	(2 0)	—
3	—	(0 1 0 0)
		(2 0 0 0)
4	—	—
5	(3 0)	(0 0 1 0)
		(1 1 0 0)
6	—	—
7	(0 1)	(0 0 0 1)
	(4 0)	(3 0 0 0)
		(1 0 1 0)
8	(1 1)	
9	—	

The computational results were produced using the open source MATLAB toolbox S-IFISS [3]. In the first instance, we run Algorithm 5.1 with Q_1 approximation with a stopping tolerance tol = 2.5e-3. We plot the energy error estimates η_k at each step $k = 0, 1, 2, \ldots$ of the algorithm as a function of the total number of degrees of freedom, $n_k = \dim\big(X(h_k) \otimes \mathcal{P}_{\mathfrak{P}_k}\big)$. The results are shown in Figure 6.1. The evolution of the index sets in these two cases (fast and slow decay) is shown in Table 6.1. This identifies the new indices that are added to the index set at steps of the adaptive algorithm where the polynomial space on Γ is enriched.

Next, we run Algorithm 5.1 with Q_2 approximation with a stopping tolerance tol = 2.5e-4. We plot the energy error estimates η_k as a function of the total number of degrees of freedom at each step $k = 0, 1, 2, \ldots$ in Figure 6.2. The evolution of the index sets is identified in Table 6.2 and is visualized as bar plots in Figure 6.3.

Looking in detail at the results in Figure 6.1 and Table 6.1, we observe that for the same level of accuracy, the final index set generated by the adaptive algorithm is larger in the case of a slower decay rate (9 indices for $\tilde{\sigma} = 2$ vs. 7 indices for $\tilde{\sigma} = 4$). We also see that more random variables are activated in the slow decay case, and that they have a lower degree of polynomial approximation (polynomials of total degree 3 in 4 random variables for $\tilde{\sigma} = 2$ vs. polynomials of degree 4 in 2 random variables for $\tilde{\sigma} = 4$). These features are even more pronounced when using Q_2 approximation. Looking at Table 6.2 and Figure 6.3 we find 65 active indices for $\tilde{\sigma} = 2$ that include polynomials of degree 5 in 13 random variables vs. 23 active indices for $\tilde{\sigma} = 4$ covering polynomials of degree 8 in 4 random variables. This behavior is consistent with what we might expect, and reflects the influence of the higher-order Fourier modes in the expansion (2.9) on the solution—this influence is more significant in the case of slow

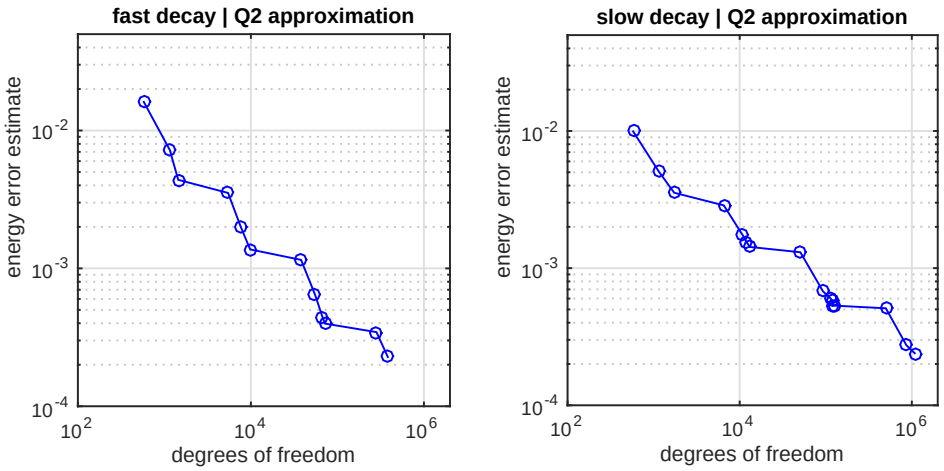

FIG. 6.2. *Error estimates at each step of the adaptive algorithm using Q_2 spatial approximation, with fast ($\tilde{\sigma} = 4$) and slow ($\tilde{\sigma} = 2$) decay of the amplitude coefficients.*

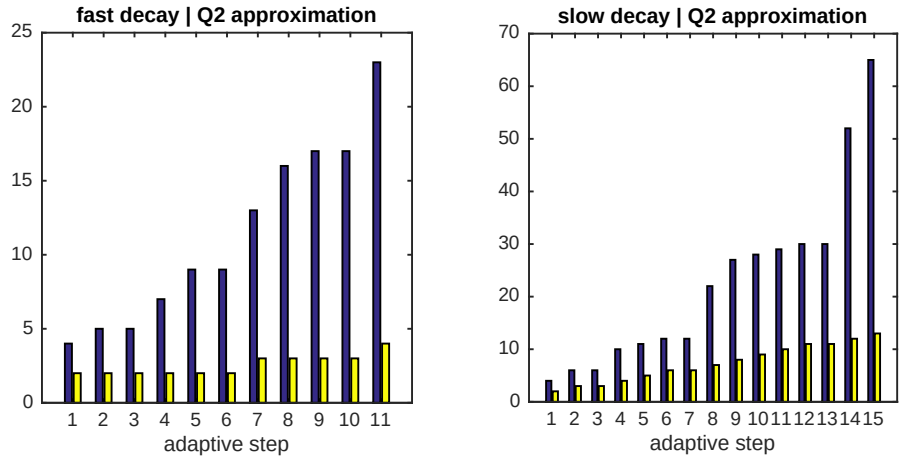

FIG. 6.3. *The number of active indices (darker bars) and active random variables (lighter bars) at each step of the adaptive algorithm with Q_2 spatial approximation.*

decay of the coefficients than in the case of fast decay.

We should emphasize the point that having a more accurate spatial approximation enables one to compute a significantly more accurate sGFEM solution. Indeed, for a comparable number of degrees of freedom the total error estimate in the sGFEM solution is smaller by up to one order of magnitude when Q_2 approximation is used in place of Q_1 approximation (check the vertical scales in Figures 6.1 and 6.2). There are two side effects of this: more steps of the algorithm are typically needed in order to reach the higher level of accuracy (over twice as many in the case of slow decay)

TABLE 6.2

Evolution of the index set at each step k of the adaptive algorithm using Q_2 approximation for fast ($\bar{\sigma} = 4$) and slow ($\bar{\sigma} = 2$) decay of the amplitude coefficients α_m. The entries '—' represent steps when a spatial refinement is performed.

k	fast decay	slow decay
0	(0 0 0 0) (1 0 0 0)	(0 0 0 0 0 0 0 0 0 0 0 0 0 0 0 0) (1 0 0 0 0 0 0 0 0 0 0 0 0 0 0 0)
1	(2 0 0 0) (0 1 0 0)	(0 1 0 0 0 0 0 0 0 0 0 0 0 0 0 0) (2 0 0 0 0 0 0 0 0 0 0 0 0 0 0 0)
2	(3 0 0 0)	(0 0 1 0 0 0 0 0 0 0 0 0 0 0 0 0) (1 1 0 0 0 0 0 0 0 0 0 0 0 0 0 0)
3	—	—
4	(4 0 0 0) (1 1 0 0)	(0 0 0 1 0 0 0 0 0 0 0 0 0 0 0 0) (3 0 0 0 0 0 0 0 0 0 0 0 0 0 0 0) (1 0 1 0 0 0 0 0 0 0 0 0 0 0 0 0) (2 1 0 0 0 0 0 0 0 0 0 0 0 0 0 0)
5	(5 0 0 0) (2 1 0 0)	(0 0 0 0 1 0 0 0 0 0 0 0 0 0 0 0)
6	—	(0 0 0 0 0 1 0 0 0 0 0 0 0 0 0 0)
7	(3 1 0 0) (6 0 0 0) (0 0 1 0) (1 0 1 0)	—
8	(4 1 0 0) (7 0 0 0) (2 0 1 0)	(1 0 0 1 0 0 0 0 0 0 0 0 0 0 0 0) (2 0 1 0 0 0 0 0 0 0 0 0 0 0 0 0) (0 0 0 0 0 0 1 0 0 0 0 0 0 0 0 0) (0 2 0 0 0 0 0 0 0 0 0 0 0 0 0 0) (1 0 0 0 0 1 0 0 0 0 0 0 0 0 0 0) (4 0 0 0 0 0 0 0 0 0 0 0 0 0 0 0) (1 0 0 0 1 0 0 0 0 0 0 0 0 0 0 0) (3 1 0 0 0 0 0 0 0 0 0 0 0 0 0 0) (0 1 1 0 0 0 0 0 0 0 0 0 0 0 0 0) (1 2 0 0 0 0 0 0 0 0 0 0 0 0 0 0)
9	(5 1 0 0)	(0 0 0 0 0 0 0 1 0 0 0 0 0 0 0 0) (2 0 0 1 0 0 0 0 0 0 0 0 0 0 0 0) (1 1 1 0 0 0 0 0 0 0 0 0 0 0 0 0) (3 0 1 0 0 0 0 0 0 0 0 0 0 0 0 0) (1 0 0 0 0 0 1 0 0 0 0 0 0 0 0 0)
10	—	(0 0 0 0 0 0 0 0 1 0 0 0 0 0 0 0)
11	(3 0 1 0) (0 0 0 1) (8 0 0 0) (6 1 0 0) (0 2 0 0) (1 2 0 0)	(0 0 0 0 0 0 0 0 0 1 0 0 0 0 0 0)
12		(0 0 0 0 0 0 0 0 0 0 0 1 0 0 0 0)
13		—
14		(0 0 0 0 0 0 0 0 0 0 0 0 1 0 0 0) (0 1 0 1 0 0 0 0 0 0 0 0 0 0 0 0) (2 0 0 0 0 1 0 0 0 0 0 0 0 0 0 0) (1 0 0 0 0 0 0 0 0 1 0 0 0 0 0 0) (2 0 0 0 1 0 0 0 0 0 0 0 0 0 0 0) (0 1 0 0 1 0 0 0 0 0 0 0 0 0 0 0) (1 0 0 0 0 0 0 1 0 0 0 0 0 0 0 0) (2 2 0 0 0 0 0 0 0 0 0 0 0 0 0 0) (2 1 1 0 0 0 0 0 0 0 0 0 0 0 0 0) (1 0 0 0 0 0 0 0 1 0 0 0 0 0 0 0) (4 1 0 0 0 0 0 0 0 0 0 0 0 0 0 0) (5 0 0 0 0 0 0 0 0 0 0 0 0 0 0 0) (0 0 2 0 0 0 0 0 0 0 0 0 0 0 0 0) (1 1 0 1 0 0 0 0 0 0 0 0 0 0 0 0) (1 0 0 0 0 0 0 0 0 0 1 0 0 0) (3 0 0 1 0 0 0 0 0 0 0 0 0 0 0 0) (0 0 1 1 0 0 0 0 0 0 0 0 0 0 0 0) (0 1 0 0 0 1 0 0 0 0 0 0 0 0 0 0) (2 0 0 0 0 0 1 0 0 0 0 0 0 0 0 0) (4 0 1 0 0 0 0 0 0 0 0 0 0 0 0 0) (0 0 1 0 0 1 0 0 0 0 0 0 0 0 0 0) (0 1 0 0 0 0 1 0 0 0 0 0 0 0 0 0)
15		(0 0 0 0 0 0 0 0 0 0 0 0 0 0 0 1) (1 1 0 0 1 0 0 0 0 0 0 0 0 0 0 0) (1 0 2 0 0 0 0 0 0 0 0 0 0 0 0 0) (2 1 0 1 0 0 0 0 0 0 0 0 0 0 0 0) (1 0 0 0 0 0 0 0 0 0 0 0 0 1 0) (1 0 1 1 0 0 0 0 0 0 0 0 0 0 0 0) (1 1 0 0 0 1 0 0 0 0 0 0 0 0 0 0) (2 0 0 0 0 0 0 0 0 1 0 0 0 0) (3 2 0 0 0 0 0 0 0 0 0 0 0 0 0 0) (3 1 1 0 0 0 0 0 0 0 0 0 0 0 0 0) (2 0 0 0 0 0 0 1 0 0 0 0 0 0 0) (3 0 0 0 0 1 0 0 0 0 0 0 0 0 0) (3 0 0 0 1 0 0 0 0 0 0 0 0 0 0)

and, as a consequence, a much richer index set is likely to be constructed (there are nearly 7 times as many active indices in the final Q_2 based approximation compared to the final Q_1 approximation in the case of slow decay). We also observe that the *rate* of convergence of the adaptive algorithm with Q_1 approximation seems to be independent of the rate of decay of coefficients (see Figure 6.1), whereas the adaptive algorithm with Q_2 approximation appears to converge slightly faster in the case of fast decay (see Figure 6.2).

TABLE 6.3

The energies, total error estimates, reference errors, and effectivity indices for the sGFEM solutions at each iteration step in the case $\tilde{\sigma} = 4$ (fast decay); in this case $\|u_{\text{ref}}\|_B$ = 1.94142e-01, $n_{\text{ref}} = 382743$.

k	n_k	$\|u_k\|_B$	η_k	$\|e_k^{\text{ref}}\|_B$	θ_k
0	578	1.92490e-01	3.18519e-02	2.52709e-02	1.26
1	2178	1.93018e-01	2.08364e-02	2.08574e-02	1.00
2	3267	1.93753e-01	1.57841e-02	1.22716e-02	1.29
3	12675	1.93893e-01	9.99149e-03	9.81808e-03	1.02
4	49923	1.93928e-01	7.97375e-03	9.10216e-03	0.88
5	66564	1.94057e-01	5.51003e-03	5.73418e-03	0.96
6	264196	1.94066e-01	4.61169e-03	5.42581e-03	0.85
7	396294	1.94114e-01	2.91629e-03	3.26522e-03	0.89
8	462343	1.94124e-01	2.54321e-03	2.64887e-03	0.96
9	1842183	1.94126e-01	2.04781e-03	2.48012e-03	0.83

To conclude the discussion we would like to demonstrate the efficiency of our error estimation strategy. To this end, we let $u_k \in X(h_k) \otimes \mathcal{P}_{\mathfrak{P}_k}$ be the Galerkin solution computed at each step $k = 0, 1, 2, \ldots$ of the adaptive algorithm with Q_1 approximation (see Table 6.1 for details of refinement at each step), and let η_k be the corresponding estimate of the energy error given by (5.4). We want to compare η_k with the energy norm of the true error $e_k := u - u_k$, where $u \in L^2_\pi(\Gamma, H^1_0(D))$ is the exact solution of our model problem. Using Galerkin orthogonality and the symmetry of the bilinear form B, we have the error representation $\|e_k\|_B^2 = \|u\|_B^2 - \|u_k\|_B^2$. A computable estimate of the energy error at the kth step may then be obtained by replacing the unknown exact solution u by an accurate (reference) solution $u_{\text{ref}} \in X(h_{\text{ref}}) \otimes \mathcal{P}_{\mathfrak{P}_{\text{ref}}}$ in the error representation. In simple terms, we approximate the energy norm of the true error by

$$\|e_k\|_B \approx \left(\|u_{\text{ref}}\|_B^2 - \|u_k\|_B^2\right)^{1/2} := \|e_k^{\text{ref}}\|_B$$

and we then compute the effectivity index given by $\theta_k = \eta_k / \|e_k^{\text{ref}}\|_B$.

Thus, given that Q_2 approximation leads to significantly increased accuracy, a suitable candidate reference solution for the Q_1 results can be generated by running the adaptive algorithm with a small error tolerance using Q_2 approximation on a fine spatial grid. In our case, $X(h_{\text{ref}})$ is defined on the uniform grid $\square_{h_{\text{ref}}}$ with $h_{\text{ref}} = 2^{-6}$, and $\mathfrak{P}_{\text{ref}}$ is the final index set when the tolerance (tol = 2.5e-04) is reached (e.g., in the case of fast decay, $\mathfrak{P}_{\text{ref}}$ is the collection of all indices in the second column in Table 6.2, and the corresponding reference solution u_{ref} is the one with the smallest error estimate plotted on the left-hand plot in Figure 6.2).

The results of these computations are presented in Table 6.3 (for $\tilde{\sigma} = 4$) and in Table 6.4 (for $\tilde{\sigma} = 2$). As the iteration converges, the effectivity indices tend to

decrease. This behavior illustrates the increasing influence of the higher-order Fourier modes in the coefficient expansion: it reflects the fact that the error estimates η_k are based on the parameter-free bilinear form B_0. It also goes without saying that the effectivity index is remarkably close to unity at every step!

TABLE 6.4

The energies, total error estimates, reference errors, and effectivity indices for the sGFEM solutions at each iteration step in the case $\tilde{\sigma} = 2$ (slow decay); in this case $\|u_{\rm ref}\|_B = 1.90117\text{e-}01$, $n_{\rm ref}$=1081665.

k	n_k	$\|u_k\|_B$	η_k	$\|e_k^{\rm ref}\|_B$	θ_k
0	578	1.89179e-01	2.29925e-02	1.88606e-02	1.22
1	2178	1.89633e-01	1.39596e-02	1.35540e-02	1.03
2	8450	1.89746e-01	1.08927e-02	1.18594e-02	0.92
3	16900	1.89996e-01	6.82414e-03	6.76065e-03	1.01
4	66564	1.90025e-01	5.21155e-03	5.89584e-03	0.88
5	99846	1.90074e-01	3.79683e-03	4.03873e-03	0.94
6	396294	1.90081e-01	3.08163e-03	3.68263e-03	0.84
7	594441	1.90100e-01	2.23643e-03	2.55596e-03	0.87

7. Concluding remarks. Adaptive algorithms are destined to play a crucial role in the computational solution of elliptic PDE problems with correlated random data. There are two very important contributions in this paper. First, the energy orthogonality that is built into stochastic Galerkin approximations can be exploited to give an innovative energy error estimation strategy that separates the contribution to the overall error coming from the spatial approximation from the part that is due to the parametric approximation. Second, our adaptive algorithm utilizes the fact that estimators corresponding to the parametric approximation can be individually probed in order to decide how to enrich the approximation space at the next adaptive step.

In contrast to previous work in this area, which typically estimates a posteriori errors by taking norms of residuals, our approach generates precise estimates of energy reductions that will occur if different refinement strategies are pursued. Extensive numerical testing confirms that effectivity indices that are close to unity can be maintained throughout the adaptive refinement process. A final distinctive feature is that our software implementation is not limited to the lowest-order conforming spatial approximation—this means that we can solve spatially-regular problems to high accuracy in an efficient manner.

REFERENCES

[1] M. AINSWORTH AND J. T. ODEN, *A posteriori error estimation in finite element analysis*, Wiley, 2000.

[2] I. BABUŠKA, R. TEMPONE, AND G. E. ZOURARIS, *Galerkin finite element approximations of stochastic elliptic partial differential equations*, SIAM J. Numer. Anal., 42 (2004), pp. 800–825.

[3] A. BESPALOV, C. POWELL, AND D. SILVESTER, *Stochastic IFISS (S-IFISS) version 1.0*, July 2015. available online at `http://www.manchester.ac.uk/ifiss/s-ifiss1.0.tar.gz` .

[4] A. BESPALOV, C. E. POWELL, AND D. SILVESTER, *Energy norm a posteriori error estimation for parametric operator equations*, SIAM J. Sci. Comput., 36 (2014), pp. A339–A363.

[5] T. BUTLER, P. CONSTANTINE, AND T. WILDEY, *A posteriori error analysis of parameterized linear systems using spectral methods*, SIAM J. Matrix Anal. Appl., 33 (2012), pp. 195–209.

[6] T. Butler, C. Dawson, and T. Wildey, *A posteriori error analysis of stochastic differential equations using polynomial chaos expansions*, SIAM J. Sci. Comput., 33 (2011), pp. 1267–1291.
[7] M. Eigel, C. J. Gittelson, C. Schwab, and E. Zander, *Adaptive stochastic Galerkin FEM*, Comput. Methods Appl. Mech. Engrg., 270 (2014), pp. 247–269.
[8] V. Eijkhout and P. Vassilevski, *The role of the strengthened Cauchy-Buniakowskiĭ-Schwarz inequality in multilevel methods*, SIAM Rev., 33 (1991), pp. 405–419.
[9] W. Gautschi, *Orthogonal polynomials: computation and approximation*, Numerical Mathematics and Scientific Computation, Oxford University Press, New York, 2004. Oxford Science Publications.
[10] R. G. Ghanem and P. D. Spanos, *Stochastic finite elements: a spectral approach*, Springer, New York, 1991.
[11] C. J. Gittelson, *An adaptive stochastic Galerkin method for random elliptic operators*, Math. Comp., 82 (2013), pp. 1515–1541.
[12] A. Keese, *A review of recent developments in the numerical solution of stochastic partial differential equations (stochastic finite elements)*, Technical Report 2003–06, Institute of Scientific Computing, TU Braunschweig, 2003.
[13] O. P. Le Maître, O. M. Knio, H. N. Najm, and R. G. Ghanem, *Uncertainty propagation using Wiener-Haar expansions*, J. Comput. Phys., 197 (2004), pp. 28–57.
[14] O. P. Le Maître, H. N. Najm, R. G. Ghanem, and O. M. Knio, *Multi-resolution analysis of Wiener-type uncertainty propagation schemes*, J. Comput. Phys., 197 (2004), pp. 502–531.
[15] O. P. Le Maître, H. N. Najm, P. P. Pébay, R. G. Ghanem, and O. M. Knio, *Multi-resolution-analysis scheme for uncertainty quantification in chemical systems*, SIAM J. Sci. Comput., 29 (2007), pp. 864–889 (electronic).
[16] Q. Liao, *Error estimation and stabilization for low order finite elements*, PhD thesis, Manchester Institute for Mathematical Sciences, The University of Manchester, Manchester, UK, 2010. Electronically published at `http://eprints.ma.man.ac.uk/1571`.
[17] C. Schwab and C. J. Gittelson, *Sparse tensor discretizations of high-dimensional parametric and stochastic PDEs*, Acta Numer., 20 (2011), pp. 291–467.
[18] P. K. Suetin, *Classical orthogonal polynomials*, "Nauka", Moscow, 1979. (in Russian).
[19] X. Wan and G. E. Karniadakis, *An adaptive multi-element generalized polynomial chaos method for stochastic differential equations*, J. Comput. Phys., 209 (2005), pp. 617–642.
[20] ———, *Error control in multi-element generalized polynomial chaos method for elliptic problems with random coefficients*, Commun. Comput. Phys., 5 (2009), pp. 793–820.